Development of Voltammetric Double-Polymer-Modified Electrodes for Nanomolar Ion Detection for Environmental and Biological Applications

by

Yushin Kim

BS, Hanyang University, 2000

MS, Hanyang University, 2002

Submitted to the Graduate Faculty of

the Kenneth P. Dietrich school of Arts and Sciences in partial fulfillment

of the requirements for the degree of

Doctor of Philosophy

University of Pittsburgh

2014

UNIVERSITY OF PITTSBURGH

DIETRICH SCHOOL OF ARTS AND SCIENCES

This dissertation was presented

by

Yushin Kim

It was defended on

April 2nd, 2014

and approved by

Stephen G. Weber, Professor, Department of Chemistry

Adrian C. Michael, Professor, Department of Chemistry

Minhee Yun, Associate Professor, Department of Electrical & Computer Engineering

Dissertation Advisor: Shigeru Amemiya, Associate Professor, Department of Chemistry

Development of Voltammetric Double-Polymer-Modified Electrodes for Nanomolar Ion Detection for Environmental and Biological applications

Yushin Kim, PhD

University of Pittsburgh, 2014

Qualitative and quantitative electrochemical methods for trace ion analysis of organic and inorganic species with environmental and biological attention have been developed and reported during past decades. The development of fast and accurate electrochemical methods is critical for field applications with various blocking contaminants. Voltammetric method is attractive not only to analyze selective ion species due to its characteristic based on ion lipophilicity, but also to lower the limit of detection by combining with stripping analysis. In my PhD work, I have developed and studied a highly selective and sensitive electrochemical method that can be used to characterize fundamental transport dynamics and to develop electrochemical sensors at liquid/liquid interfaces based on electrochemically-controlled ion transfer and recognition. The understanding of the kinetic and thermodynamic properties of the voltammetric ion transfer through polymer-modified ion-selective electrodes leads to realize the highly selective and sensitive analytical method. The ultrathin polymer membrane is used to maximize a current response by complete exhaustion of preconcentrated ions. Therefore, nanomolar detection is achieved and confirmed by a thermodynamic mechanism that controls the detection limit. It was also demonstrated experimentally and theoretically that more lipophilic ionic species gives a significantly lower detection limit. The voltammetric method was expanded into inexpensive and disposable applications based on pencil lead modified with the thin polymer membrane. In the other hand, micropipet/nanopipet voltammetry as an artificial cell membrane was used to study

the interface between two immiscible solutions for environmental and biomedical applications. It is very useful to get quantitative kinetic and thermodynamic information by studying numerical simulations of ion transfer and diffusion. Molecular recognition and transport of heparin and low-molecular-weight heparin drove by hydrophobic receptors were examined thermodynamically and demonstrated that the selectivity for sensor applications is influenced by the interfacial interactions. Also, we found that a new heparin ionophore enables voltammetric extraction of heparins with various average molecular weights.

TABLE OF CONTENTS

LIST OF TABLES

LIST OF FIGURES

LIST OF SCHEMES

LIST OF EQUATIONS

ACKNOWLEDGEMENTS

I would like to express my sincere gratitude to my advisor, Professor Shigeru Amemiya, for the training that he has provided during my graduate program. Professor Amemiya has invested a tremendous amount of time and energy to help me to develop into a professional scientist. I greatly appreciate his contributions to my success.

I want to thank Professor Adrian Michael, Professor Stephen Weber and Professor Minhee Yun for their willingness to serve on my dissertation committee. I value my interaction with each of them, which has been beneficial for my development and continued success in my scientific career.

I want to acknowledge the former and past members of the Amemiya research group for their support and encouragement. I am thankful for their scientific contributions and friendship.

I also want to acknowledge my family, friends and colleagues. Their consistent support through successful and challenging periods during my graduate program is invaluable.

Finally, I want to give special honor to my wife, Sangmi. She has sacrificed so much of our time together so that I could be successful in this program. Thank you for supporting me through my graduate program, which demanded so much of me.

1.0 INTRODUCTION

In my PhD work, I have developed and studied a highly selective and sensitive electrochemical method that can be used to characterize fundamental transport dynamics and to develop electrochemical sensors at liquid/liquid interfaces based on electrochemically-controlled ion transfer and recognition. In the first chapter, a highly selective analytical method based on a voltammetric ion-selective electrode is developed to detect perchlorate at nanomolar level in drinking water for an emerging environmental contamination problem. The perchlorate-selective electrode with the low detection limit based on thin polymer membrane supported with a conducting polymer modified solid electrode is enabled by ion-transfer stripping voltammetry under rotating electrode configuration. The ultrathin polymer membrane serves as the first thin-layer cell to maximize a current response by complete exhaustion of preconcentrated perchlorate during stripping step, which is validated by theoretical models. The developed electrochemical method is utilized in Chapter 3. Herein, we demonstrate experimentally and theoretically that more lipophilic ionic species gives a significantly lower detection limit for both cationic and anionic species. Chapter 4 highlights the inexpensive and disposable electrode based on pencil lead modified with the thin polymer membrane. The simple electrodes allow detecting perchlorate in drinking water with a linear current response to 100-1000 nM, which is below an interim health advisory level set by the U.S Environmental Protection Agency. Chapter 5 and 6 present the investigation of voltammetric extraction of heparin and low-molecular-wight heparin

by micropipet voltammetry. Based on a greater understanding of interfacial recognition and sensing of heparin, we found that a new heparin ionophore enables voltammetric extraction of heparins with various average molecular weights. By full characterization of facilitated heparin extration, we suggest that cooperative effects from strong binding capability and high lipophilicity of this ionophore are required for the formation of a neutral and lipophilic complex of a heparin molecule with multiple ionophore molecules, which indicate the importance of ionophore design. My contributions in this work include designing and synthesizing ionophores.

2.0 STRIPPING ANALYSIS OF NANOMOLAR PERCHLORATE IN DRINKING WATER WITH A VOLTAMMETRIC ION-SELECTIVE ELECTRODE BASED ON THIN-LAYER LIQUID MEMBRANE

This work has been published as Y. Kim and S. Amemiya, *Anal. Chem.,* **2008**, *80*, 6056-6065.

2.1 INTRODUCTION

Public concern about perchlorate in the environment has steadily increased in recent years.[1] In addition to its natural existence, perchlorate is widely used as an oxidant in solid rocket fuel, matches, fireworks, automobile airbag-inflation systems, and a variety of other industrial applications including the production of dyes, paints, and rubber.[2] Recently, the trace amount of perchlorate (1-100 ppb, i.e., ~10-1000 nM) was found in drinking water,[2] human and cow's milk,[3] and produce.[4] The potential health effects associated with perchlorate include the disruption of the thyroid function.[5] The active uptake of iodide in the thyroid as mediated by Na^+/I^- symporter is blocked or competes with perchlorate.[6,7] The resulting reduced production of iodine-containing thyroid hormones can impair the gland development as seen in the conditions of hypothyroidism or hypothyroxinemia. Pregnant women, children, and people with a

compromised thyroid function are particularly at risk. Currently, the U.S. Environmental Protection Agency (EPA) sets the action limit of 24.5 ppb (~246 nM) perchlorate in drinking water.[8]

Only a few of the various methods of perchlorate analysis[9] are sensitive enough for the trace analysis of perchlorate in drinking water samples. Ion chromatography with a suppressed conductivity detector has been recommended by the EPA (Methods 314.0[10] and 314.1[11]). Two-dimensional ion chromatography lowers the detection limit of perchlorate to 55 ng/L (~0.55 nM).[12] Electrospray ionization mass spectrometry (ESI-MS), which requires ^{18}Oenriched perchlorate as an internal standard, is also employed as the detector of liquid or ion chromatography (Method 331.0[13] or 332.0,[14] respectively). The detection limit by ESI-MS can be lowered to 20-25 ng/L (~0.20-25 nM) by introducing a dicationic postcolumn reagent, which forms the positively charged complex with a perchlorate molecule in the gas phase to increase the selectivity and sensitivity of the ESI-MS detection.[15,16] On the other hand, direct spectroscopic and electrochemical approaches, which are desirable as the field methods of trace perchlorate analysis, suffer from low sensitivity. Raman scattering gives a detection limit of only 1 μg/mL, while colorimetry or spectrophotometry usually requires the ion-pair extraction of perchlorate and dye molecules.[9] The perchlorate reduction at a solid electrode is the slow process based on a complicated stepwise mechanism, thereby rendering perchlorate kinetically redox-inactive.[17] The conductive polypyrrole film coated on a solid electrode was used only for the electrochemical sampling of perchlorate, which was detected by ESI-MS.[18]

During the past decade, potentiometry with liquid-membrane ion-selective electrodes (ISEs) has been extensively explored to enable the electrochemical detection of trace ions without their electrolysis.[19] The transmembrane flux of an analyte ion from the internal solution

to the sample solution was discovered as the origin of biased detection limits.[20] Several approaches to lower the detection limits by the control of the transmembrane ion flux have been developed for various ions.21 In fact, a detection limit of 18 nM perchlorate in deionized water was obtained by potentiometry using the plasticized poly(vinyl chloride) (PVC) membrane doped with lipophilic quaternary ammoniums as anion exchangers.[22] The potentiometric perchlorate-selective electrode, however, possesses a much higher detection limit than the EPA methods and has not been applied for the analysis of real samples. Moreover, potentiometric ISEs generally give a nonequilibrium response[23] to an analyte ion at a low activity, which is readily depleted at the membrane/sample solution interface by exchange[21] or coextraction[24] with an interfering ion. The resulting nonequilibrium response compromises not only a detection limit[25] but also the selectivity because of the convoluted response to both analyte and interfering ions. Slower interfacial equilibration at a lower analyte activity results in a prolonged response time of even a few hours.[21,25]

Here we report on a voltammetric ISE with low detection limits of 0.2-0.5 nM perchlorate in deionized water, commercial bottled water, and tap water. Specifically, the submicrometer-thick plasticized PVC membrane spin-coated on the poly(3-octylthiophene) (POT)-modified gold electrode (Figure 1)[26] is operated in the mode of ion-transfer stripping voltammetry[27] under a rotating electrode configuration. In contrast to conventional stripping voltammetry based on the redox reaction of an analyte at a mercury or a solid electrode, [28]ion-transfer stripping voltammetry enables the detection of perchlorate without its electrolysis. With this operation mode, a constant anodic potential is externally applied to the gold electrode such that aqueous perchlorate is preconcentrated into the thin PVC membrane while the underlying POT film is oxidized to mediate the charge transport between the ionically conductive PVC

membrane and electronically conductive gold electrode (Figure 1a). After this preconcentration step, the potential is swept to the cathodic direction such that the reduction of the oxidized POT film is coupled with stripping of the concentrated perchlorate molecules from the membrane phase into the aqueous sample to obtain the enhanced ionic current response (Figure 1b). In comparison to previous studies by us[26,29] and others,[30–45] the thinner liquid membrane spin-coated on a solid support serves as the first thin-layer cell for ion-transfer stripping voltammetry to maximize the stripping current response by the total exhaustion of the preconcentrated perchlorate molecules from the membrane. Theoretical models are developed and validated experimentally to assess the diffusion and preconcentration of perchlorate in the thinlayer liquid membrane. This stripping approach offers advantages against traditional ion-selective potentiometry in a detection limit, a response time, and selectivity.

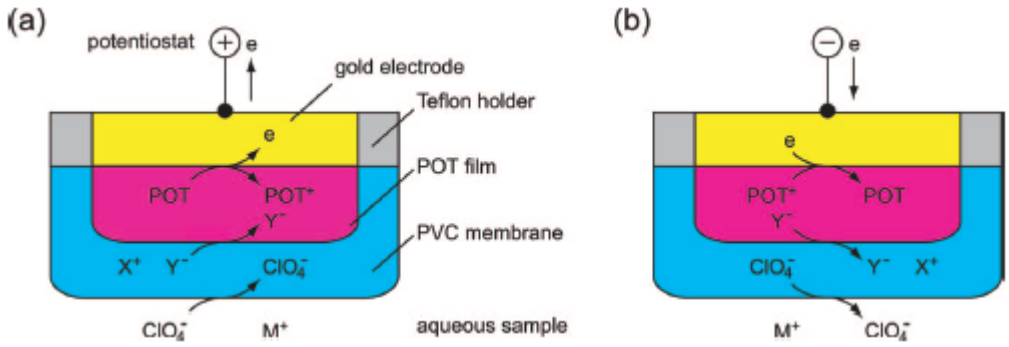

Figure 2-1. Scheme of ion-transfer stripping voltammetry with the thin PVC membrane coated on the POT-modified gold electrode for (a) the preconcentration and (b) the stripping (detection) of perchlorate. X+ and Y- are organic supporting electrolytes while M+ is an aqueous cation.

2.2 THEORY

2.2.1 Model

A theoretical model was developed to quantitatively assess ion diffusion in a solid-supported liquid membrane by cyclic voltammetry. The model is analogous to that of a thin mercury film electrode.[46,47] The diffusion problem based on the model was solved using COMSOL Multiphysics version 3.4 (COMSOL, Inc., Burlington, MA), which applies the finite element method. The simulation accuracy of this software package for two-phase diffusion processes was demonstrated previously.[48,49] Calculation of each CV took <10 s on a workstation equipped with a Xeon 3.0 GHz processor unit and 5.0 GB RAM with Linux. The original and dimensionless forms of the problem and the example of a numerical simulation are available as Supporting Information.

The geometry of the liquid membrane sandwiched between an aqueous solution and a solid electrode is defined in a linear coordinate, *x*, vertical to the interfaces. An ion with the charge z^i, i^{z_i}, is initially present only in the aqueous solution. The simple transfer of the ion is defined by

Equation 2-1 i^{z_i} **(aqueous phase)** $\rightleftharpoons$ i^{z_i} **(membrane phase)**

The current based on this ion transfer, *i*, was numerically calculated by solving the diffusion problem and normalized against the peak current on the forward scan, i_{pa}. The simulated peak current agrees with the value expected for the reversible voltammogram based on semi-infinite linear diffusion as given by[50]

Equation 2-2

$$i_{pa} = 0.4463\left(\frac{F^3}{RT}\right) z_i^{3/2} A\sqrt{D_w} c_0 \sqrt{v}$$

where F is Faraday's constant, A is the interfacial area, D_w and c_0 are the diffusion coefficient and concentration of the ion in the bulk aqueous phase, respectively, and v is the potential sweep rate. The normalized current, i/i_{pa}, was plotted with respect to $|z_i|\Delta\phi$, where $\Delta\phi$ is the overpotential at the liquid membrane/sample solution interface defined as

Equation 2-3

$$\Delta\phi = \Delta_w^m\phi - \Delta_w^m\phi_i^{0'}$$

where $\Delta_w^m\phi$ is the Galvani potential difference between the membrane and aqueous phases, and $\Delta_w^m\phi_i^{0'}$ is the formal ion transfer potential at the membrane/water interface.

2.2.2 Cyclic Voltammetry at Thin Liquid Membranes

The diffusion problem was solved for the nernstian transfer of an anion at the interface between the liquid membrane and sample solution (Figure 2a). The wave shape on the anodic potential sweep is identical with the shape of the reversible wave based on the semi-infinite linear diffusion of transferred ions in both membrane and aqueous phases.[50] On the other hand, the wave shape on the following cathodic potential sweep strongly depends on the dimensionless parameter, σ, given by

Equation 2-4

$$\sigma = \frac{l^2}{D_m}\frac{|z_i|Fv}{RT}$$

where l is the membrane thickness and D_m is the diffusion coefficient of the ion in the membrane phase. This dimensionless parameter is equivalent to the square of the ratio of the membrane thickness with respect to $(D_m RT/|z_i|Fv)^{1/2}$, which represents the diffusion distance of the ion in

the membrane during a potential cycle. With $\sigma \geq 100$, i.e., $l \geq 10(D_m RT/|z_i|Fv)^{1/2}$, the diffusion distance is much smaller than the membrane thickness so that the nernstian CV is controlled by the semi-infinite linear diffusion of the ion in both phases (red line in Figure 2a). With a smaller σ value of 10 (green line), the diffusion of the transferred ions in the membrane is hindered by the solid support, thereby resulting in the larger cathodic peak current. The cathodic peak current becomes even larger with $\sigma = 1$ (magenta line), where the membrane serves as a thin layer cell. The cathodic peak based on thin layer behavior is sharper and also shifts toward anodic potentials so that the separation between the anodic and cathodic peak potentials becomes narrower. A further decrease of σ to 0.1 (green line) results in the anodic shift of a whole CV while its shape is identical in this regime of thin layer behavior ($\sigma \leq 1$). Overall, a σ value can be determined uniquely from the shape of a reverse wave in the intermediate regime with $1 < \sigma < 100$.

The ratio of diffusion coefficients in the aqueous and membrane phases, i.e., $\gamma = D_w/D_m$, affects the position of a nernstian CV. This ratio is much larger than 1 with the viscous plasticized PVC membrane[51] used in this work. A CV shifts toward the anodic direction by $30/z^i$ mV for every decade decrease in γ while the CV shape is independent of γ and is determined only by σ (Figure 2b with $\sigma = 0.1$). It should also be noted that the current response varies with the square root of σ and γ, which depend on v and D_w, respectively. These dependences are not seen in parts a or b of Figure 2, where the current response is normalized against the anodic peak current, i_{pa} (eq 2).

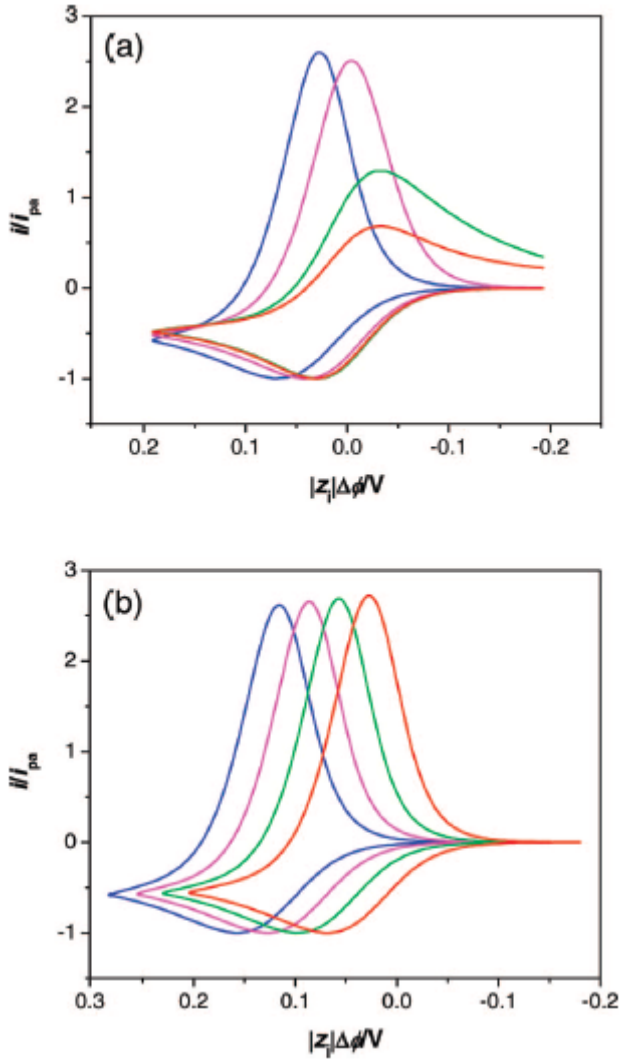

Figure 2-2. Simulated CVs based on the nernstian transfer of an anion at the membrane supported with a solid electrode for (a) γ = 1 and σ = 100 (red), 10 (green), 1 (magenta), and 0.1 (blue) and (b) σ = 0.1 and γ = 1 (red), 10 (green), 100 (magenta), and 1000 (blue).

2.3 EXPERIMENTAL SECTION

2.3.1 Chemicals

Tetradodecylammonium (TDDA) bromide and 3-octylthiophene (97%) were obtained from Aldrich (Milwaukee, WI). Poly(vinyl chloride) (PVC, high molecular weight) and 2-nitrophenyl octyl ether (oNPOE) were from Fluka (Milwaukee, WI). Potassium tetrakis-(pentafluorophenyl)borate (TFAB) was from Boulder Scientific Company (Mead, CO). All reagents were used as received. TDDA-TFAB was prepared as reported elsewhere.[26]

2.3.2 Electrode Modification

The 5 mm diameter gold disk attached to a rotating disk electrode tip (Pine Research Instrumentation, Raleigh, NC) was chemically modified as follows. The gold electrode was polished over polishing cloths containing the dispersions of alumina (0.3 and 0.05 μm, Buehler, Lake Bluff, IL) in water and cleaned by ultrasonication in concentrated dichromic acid and then in water for 15 min three times. The poly(3-octylthiophene) film that is not readily soluble in THF during spincoating of a PVC membrane was deposited on the polished electrode by cyclic voltammetry[26] using a three-electrode cell with a Ag/Ag^+ reference electrode (CH Instruments) and a Pt-wire counter electrode. The film deposition was conducted in an acetonitrile solution containing 0.1 M 3-octylthiophene and 0.5 M $LiClO_4$ by cycling the potential between 0 and 1.22 at 0.1 V/s three times using a computer-controlled CHI 600A electrochemical workstation

(CH Instruments). The final potential was set to 0 V to obtain a neutral POT film. The modified gold electrode was soaked in acetonitrile for 30 min and then in THF for 1 min to remove the soluble fractions of the POT film.

A PVC membrane was spin-coated on the 5 mm diameter gold disk modified with a POT film. A 30 μL membrane cocktail with the composition of 4 mg of PVC, 16 mg of o-NPOE, and 2.2 mg of TDDATFAB in 1 mL of THF was injected onto the gold disk rotated at 1500 rpm in a spin-coating device (model SCS-G3-8, Cookson Electronics, Providence, RI). The modified gold disk was removed from the spin coater and dried in the air for 30 min.

2.3.3 Electrochemical Measurement

The CHI 600A electrochemical workstation was used also for voltammetric measurements with the solid-supported ISEs. A three-electrode arrangement with a Ag/AgCl reference electrode (CH Instruments) and a Pt-wire counter electrode was employed. An electrochemical cell is as follows:

$$Ag|AgCl|\ KCl\ (3M)||x\ M\ LiClO_4\ in\ 0.1\ M\ Li_2SO_4\ (aq)|PVC\ membrane|POT|Au$$

The current carried by a positive charge from the aqueous phase to the PVC membrane is defined to be positive. All electrochemical experiments were performed at 22 ± 3 °C. The perchlorate concentrations are given in the Results and Discussion. Aqueous sample solutions were prepared with 18.3 MΩ cm deionized water (Nanopure, Barnstead, Dubuque, IA), tap water, or commercial bottled water. The tap water sample was collected from the cold water tap of a laboratory sink after the water was allowed to run for 15 min.

A Teflon tube with a cylindrical hole was put on the modified gold electrode tip for cyclic voltammetry under a stationary condition to obtain a disk-shaped PVC membrane/water

interface with a diameter of 1.5 mm and an interfacial area of 0.0177 cm^2. The tube was not used for cyclic voltammetry or stripping voltammetry when the electrode was rotated by using a modulated speed rotator (Pine Research Instrumentation).

2.4 RESULT AND DISCUSSION

2.4.1 Thin-Layer Liquid Membrane for Ion-Transfer Stripping Voltammetry

This work is the first to demonstrate the thin-layer behavior of a liquid membrane for ion-transfer stripping voltammetry. The potential advantages of such a thin-layer liquid membrane are analogous to the well-established advantages of a thin mercury film electrode in anodic stripping voltammetry.[52,53] The efficient diffusion of analyte ions in a thin-layer liquid membrane allows for exhaustively stripping the analyte ions from the membrane into the sample solution, thereby maximizing the current sensitivity. In addition, the stripping current response based on the total exhaustion of a thin-layer membrane has been considered to increase linearly with the duration of a preconcentration step.[42] On the other hand, the semi-infinite linear diffusion of analyte ions in a thicker membrane results in the square-root dependence of the stripping current response on the preconcentration time.[34] Also, the diffusive depletion in a thicker membrane gives a broader stripping voltammogram with compromised sensitivity and selectivity.[54]

Our solid-supported voltammetric ISE (Figure 1) is designed so that the stripping current response based on thin layer behavior is obtained despite slow ion diffusion in a viscous PVC membrane. In this setup, thin layer behavior is observed at practical potential sweep rates by using a submicrometer-thick PVC membrane while the ion-to-electron transduction between the

membrane and solid support is mediated by the intermediate POT film. In contrast, the conventional solid-supported PVC membrane doped with redox mediators must be much thicker to sustain the substantial ionic current coupled with the electrolysis of the mediators at the membrane/solid interface, thereby resulting in the semi-infinite linear diffusion of analyte ions in the membrane phase.[45] Importantly, a plasticized PVC membrane is robust enough to be rotated at fast rates so that the hydrodynamically enhanced mass transfer of analyte ions in the sample solution accelerates the analyte preconcentration. On the other hand, the mediator-doped organic solution interposed between a solid electrode and an aqueous solution is much less stable mechanically and has not been employed for ion-transfer stripping voltammetry although fast ion diffusion in the fluid organic phase with a thickness of tens of micrometers gives thin layer behavior.[55] In this work, we also demonstrate that the efficient mass transfer in the thin-layer PVC membrane and sample solution in our voltammetric setup facilitates the theoretical analysis of the stripping response.

Currently, the drawback of the voltammetric ISE based on a solid-supported liquid membrane is that the potential applied to the solid electrode, E_{app}, is distributed not only to the liquid membrane/sample solution interface but also to the liquid membrane/solid junction.[26,56] In the case of our double-polymer system, the applied potential is distributed as given by[26]

Equation 2-5 $$E_{\text{appl}} = \Delta^{\text{Au}}_{\text{PVC}}\phi + \Delta^{\text{PVC}}_{\text{w}}\phi - E_{\text{ref}}$$

where $\Delta^{\text{Au}}_{\text{PVC}}\phi$ is the potential drop at the PVC/POT/gold junction, $\Delta^{\text{PVC}}_{\text{w}}\phi$ is the phase boundary potential at the PVC membrane/sample solution interface, and E_{ref} is the reference electrode potential. The limited redox capacity of the POT film results in a substantial $\Delta^{\text{Au}}_{\text{PVC}}\phi$ value, although the charge transport at the junction is reversible.[26]

The convolution[26] and numerical (see below) analyses of CVs at our voltammetric ISEs demonstrate that both $\Delta_{\mathrm{w}}^{\mathrm{PVC}}\phi$ and $\Delta_{\mathrm{PVC}}^{\mathrm{Au}}\phi$ varies linearly with E_{app} during a potential sweep. Thus, the applied potential can be scaled to the potential at the PVC membrane/sample solution interface as

Equation 2-6
$$\Delta_{\mathrm{w}}^{\mathrm{PVC}}\phi - \Delta_{\mathrm{w}}^{\mathrm{PVC}}\phi_i^{0'} = (E_{\mathrm{app}} - E_{\mathrm{app}}^{0'})\frac{\partial\Delta_{\mathrm{w}}^{\mathrm{PVC}}\phi}{\partial E_{\mathrm{app}}}$$

where $\Delta_{\mathrm{w}}^{\mathrm{PVC}}\phi_i^{0'}$ is the formal ion-transfer potential at the PVC membrane/water interface and $E_{\mathrm{app}}^{0'}$ is the applied potential at $\Delta_{\mathrm{w}}^{\mathrm{PVC}}\phi = \Delta_{\mathrm{w}}^{\mathrm{PVC}}\phi_i^{0'}$ and can be determined from a nernstian CV with the knowledge of γ. The variation of $\partial\Delta_{\mathrm{w}}^{\mathrm{PVC}}\phi / \partial E_{\mathrm{app}}$ among different electrodes and during repeated measurements, however, compromises the reproducibility of the actual potential at the membrane/sample solution interface. Despite this complication, the actual potential must be controlled precisely in stripping voltammetry when equilibrium is reached during a preconcentration step (see below).

2.4.2 Demonstration of Thin-Layer Behavior by Cyclic Voltammetry

The diffusion of perchlorate in the spin-coated PVC membrane was assessed quantitatively by cyclic voltammetry to demonstrate thin-layer behavior. The results of finite element simulations in the Theory section predict that a liquid membrane serves as a thin layer cell in cyclic voltammetry when σ in eq 4 is equal to or smaller than 1. The slow ion diffusion in the viscous PVC membrane requires a thin membrane for satisfying $\sigma \leq 1$.

The transfer of perchlorate at the PVC membrane spin-coated on the POT-modified gold electrode was studied by cyclic voltammetry at 1 and 0.1 V/s (parts a and b of Figure 3,

respectively). The cathodic peak current is larger than the anodic one even at 1 V/s, where the diffusion of perchlorate in the thin membrane is hindered by the solid support. As v decreases to 0.1 V/s, the cathodic peak current is further enhanced to be nearly doubled with respect to the anodic one. Both CVs at 1 and 0.1 V/s fit well with the simulated nernstian CVs, thereby yielding σ = 4.2 and 0.42, D_w = 1.9 × 10^{-5} and 1.7 × 10^{-5} cm^2/s, and $\partial\Delta_w^{PVC}\phi / \partial E_{app}$ = 0.65 and 0.60, respectively. Importantly, $\sigma < 1$ is required for the good fit of the CV at 0.1 V/s, indicating that the spincoated PVC membrane serves as a thin layer cell at 0.1 V/s. In fact, the cathodic peak based on the total exhaustion of the thinlayer PVC membrane at 0.1 V/s is sharper than the cathodic peak based on the rather diffusive depletion at 1 V/s.

The thickness of the spin-coated PVC membrane was also estimated from the CV at 1 V/s to be 0.72 μm using eq 4 with the σ value and Dm) 5.0 × 10^{-8} cm^2/s (see Supporting Information). While the spin-coated membrane is only ~4 times thinner than the conventional drop-cast membrane with 3 μm thickness,[26] the corresponding σ value is ~16 times smaller for the former membrane (eq 4) to give thin layer behavior at the practical potential sweep rate of 0.1 V/s. Also, the good agreements of the experimental CVs with the CVs simulated for a homogeneous membrane confirm the negligible distribution of perchlorate into the underlying POT film during a potential cycle at 0.1-1 V/s.

As predicted theoretically (Figure 2b), the CVs are dislocated anodically with respect to $\Delta_w^{PVC}\phi_{ClO_4^-}^{0'}$, because of the much slower diffusion of perchlorate in the membrane than in the aqueous sample ($\gamma = D_w/D_m$ = 3.4 × 102). The overpotential, $\Delta\phi$, defined as the difference between $\Delta_w^{PVC}\phi$ and $\Delta_w^{PVC}\phi_{ClO_4^-}^{0'}$ was obtained from the apparent overpotential of $E_{app} - E_{app}^{0'}$ using eq 6 with the $E_{app}^{0'}$ and $\partial\Delta_w^{PVC}\phi / \partial E_{app}$ values determined from the numerical simulations (see the

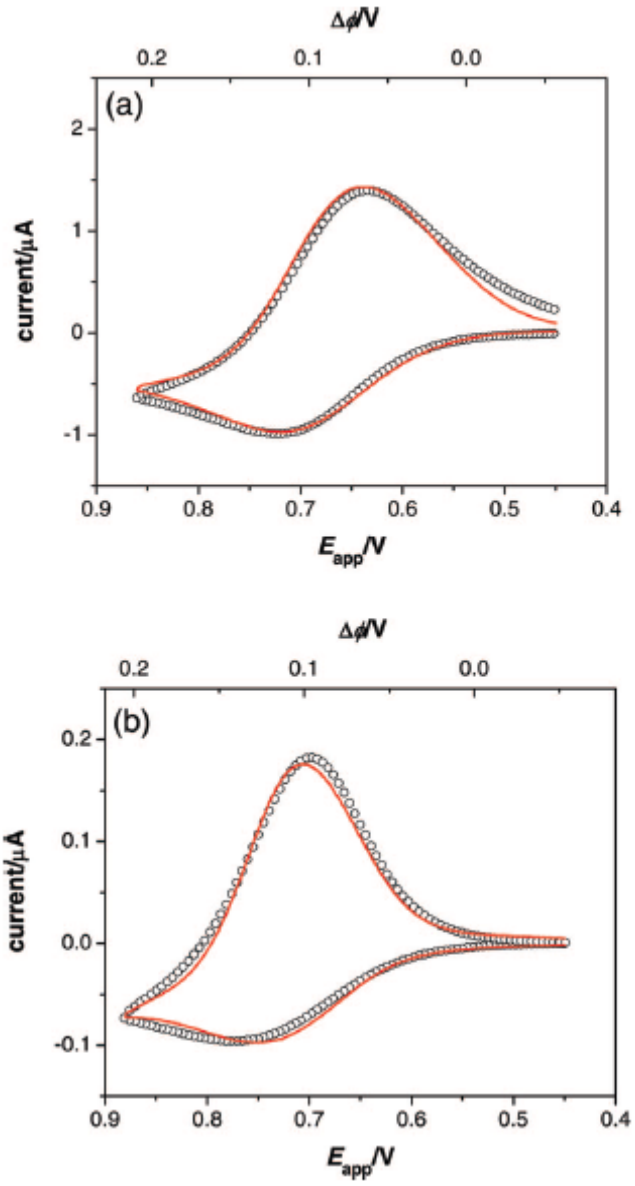

Figure 2-3. Experimental (red line) and simulated (O) CVs of perchlorate with the PVC membrane spin-coated on the POT-modified gold electrode at scan rates of (a) 1 and (b) 0.1 V/s with 60 and 20 μM $LiClO_4$, respectively.

top of Figures 3 and 10). A larger anodic offset was observed with the spin-coated PVC membrane at 0.1 V/s, where both anodic and cathodic peaks appeared at $\Delta\phi$ > 0.1 V (Figure 3b). This result confirms the theoretical prediction that a smaller σ value in the thin-layer regime results in the anodic shift of a CV (Figure 2a). Moreover, the actual overpotential is smaller than the corresponding apparent overpotential. The $\partial\Delta_{w}^{PVC}\phi / \partial E_{app}$ values indicate that only 60-65 % of the apparent overpotential contributes to the corresponding actual overpotential at the PVC membrane/sample solution interface (eq 6). In Figure 3b, for instance, $\Delta\phi$ = 0.22 V at E_{app} = 0.9 V, which corresponds to an apparent overpotential of 0.36 V with $E_{app}^{0'}$ = 0.54 V.

2.4.3 Hydrodynamically Enhanced Mass Transfer

A voltammetric perchlorate-selective electrode was rotated to hydrodynamically enhance the mass transfer of perchlorate between the sample solution and membrane surface. The faster mass transfer of aqueous perchlorate accelerates its preconcentration into the PVC membrane to lower the detection limit in ion-transfer stripping voltammetry.

We investigated the effects of electrode rotation on the CVs at the PVC membrane spin-coated on the POT-modified gold electrode. A current response increased as the electrode was rotated faster (Figure 4). The enhanced current response on the anodic potential sweep is due to the faster mass transfer of aqueous perchlorate. The sigmoidal shape of the anodic wave indicates the steady-state mass transfer of aqueous perchlorate, although the current response still increases gradually toward the switching potential. The limiting current, i_l, as defined at E_{app} = 0.9 V is proportional to the square root of the angular frequency of electrode rotation, ω (the inset of Figure 4) as expected from the Levich equation[57]

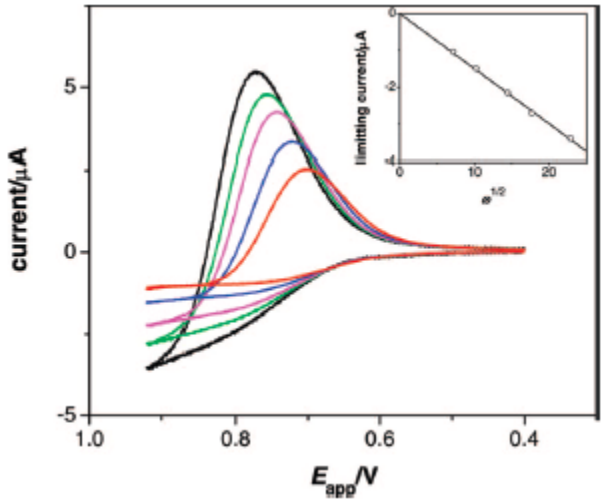

Figure 2-4. Rotating-electrode CVs of 10 μM perchlorate at the PVC membrane spin-coated on the POT-modified gold electrode at 0.1 V/s. The electrode was rotated at 500 (red), 1000 (blue), 2000 (magenta), 3000 (green), and 5000 (black) rpm. The inset shows the plot of the limiting current versus the square root of the angular frequency of electrode rotation, ω.

Equation 2-7 $$i_l = 0.62 z_i F A D_w^{2/3} \omega^{1/2} \nu^{-1/6} c_0$$

where ν is the kinematic viscosity. A slope of 1.7×10^{-7} A/s$^{1/2}$ in the plot of i_l versus $\omega^{1/2}$ corresponds to A = 0.21 cm^2 in eq 7 with c_0 = 10 μM and $\nu = 1 \times 10^{-2}$ cm^2/s. This area is much smaller than the area of the spin-coated PVC membrane (1.0 cm^2) but agrees with the area of the underlying POT film (0.19 cm^2). These results indicate that the redox reaction of the POT film limits the transfer of perchlorate spatially through the thin PVC membrane.

The current response on the cathodic potential sweep is also larger at a faster rotation rate, where the faster mass transfer of aqueous perchlorate enhances its accumulation in the membrane phase. The enhancement of the cathodic current response is not relevant to the mass transfer of perchlorate in the thin-layer PVC membrane, which is negligible and is not affected by the electrode rotation because of the high membrane viscocity.[58] In fact, the asymmetric hydrodynamic effect on the mass transfer of perchlorate in the membrane and aqueous phases results in the anodic shift of a CV at a faster rotation rate (Figure 4) although this anodic shift is partially due to larger polarization at the PVC/POT/gold junction with a larger current flow.[26]

2.4.4 Effects of Preconcentration Time on Stripping Responses

We investigated how the preconcentration time affects the stripping current response, which is expected to be proportional to the amount of the analyte ions preconcentrated in the thin-layer membrane.[42] An important finding is that the efficient mass transfer of perchlorate in the thin-layer membrane and sample solution results in equilibrium preconcentration. The equilibrium membrane concentration of perchlorate depends on its sample concentration and the overpotential at the PVC membrane/sample solution interface as governed by the Nernst equation.

The effects of preconcentration time on the stripping voltammetric response were studied under a rotating electrode configuration. In all stripping voltammetric experiments reported in this work, the applied potential was set near the anodic limit of a potential window during a preconcentration step and then swept toward the cathodic direction at 0.1 V/s, which is slow enough to totally exhaust perchlorate from a thin-layer PVC membrane. A stripping current response was clearly observed with 100 nM perchlorate after 10 s preconcentration and grew as the preconcentration time increased to 1 min (Figure 5), while no current response to 100 nM perchlorate was observed by cyclic voltammetry. The stripping current response, however, saturated after 2 min preconcentration in contrast to the assumption of the diffusion-limited preconcentration made in a previous theory.[42] This saturation is not due to the exhaustion of perchlorate from the sample solution, which possesses a much larger volume of 30 mL than a membrane volume of 14 nL.

The saturation of a liquid membrane with perchlorate molecules indicates their equilibrium partition between the membrane and sample phases during a preconcentration step. A similar equilibrium preconcentration mechanism was reported recently for anodic stripping voltammetry with a thin mercury film electrode.[59,60] The efficient ion diffusion in a thin-layer membrane results in the homogeneous membrane concentration of transferred ions, which causes the saturation. During the preconcentration step based on nernstian ion transfer, the membrane ion concentration, $c_{\mathrm{m}}(t)$, is given by the Nernst equation as

Equation 2-8

$$\frac{c_{\mathrm{m}}(t)}{c_{\mathrm{w}}(0,t)} = \exp\left[-\frac{z_{\mathrm{i}}F(\Delta_{\mathrm{w}}^{\mathrm{m}}\phi^{\mathrm{p}} - \Delta_{\mathrm{w}}^{\mathrm{m}}\phi_{\mathrm{i}}^{0'})}{RT}\right] = Y$$

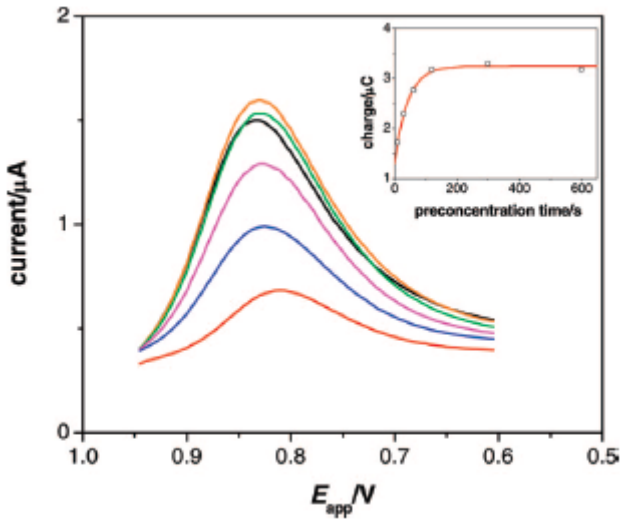

Figure 2-5. Stripping voltammograms of 100 nM perchlorate at 0.1 V/s after a preconcentration step of 10 (red), 30 (blue), 60 (magenta), 120 (green), 300 (orange), and 600 (black) s. The inset shows the plot of Q_s versus t_p, where the O and solid line represent experimental and theoretical (eq 13) values, respectively. The electrode was rotated at 4000 rpm.

where $c_w(0,t)$ is the ion concentration at the aqueous side of the interface, $\Delta_w^m\phi^p$ is the potential applied at the sample solution/PVC membrane interface during the preconcentration step, and *Y* is the preconcentration ratio.[59] Equation 8 indicates that a constant, finite potential can drive the ion transfer to a mass-transfer limitation, i.e., $c_w(0,t) \approx 0$ only when the membrane ion concentration is sufficiently low. As more ions are accumulated in the thin-layer membrane, $c_w(0,t)$ also increases to maintain the constant preconcentration ratio, *Y*, thereby resulting in a smaller ion flux from the bulk water phase to the membrane surface. At equilibrium, $c_w(0,t) = c_0$ so that $c_m(t) = c_0 Y$ and the ion flux is zero. The total charge of the preconcentrated perchlorate molecules at the equilibrium, Q_{eq}, is given by

Equation 2-9 $$Q_{eq} = z_i FAlc_0 Y$$

The potential sweep that follows the equilibrium preconcentration step gives the maximum stripping current response, which is proportional to Q_{eq}.

Equation 9 predicts that the membrane thickness and preconcentration potential significantly affect the sensitivity of the stripping current response coupled with equilibrium preconcentration in a thin-layer membrane. A thinner membrane has a lower total capacity for analyte ions because Q_{eq} is proportional to the membrane thickness. On the other hand, the membrane must be thin enough to give thin-layer behavior. Thus, the optimum thickness of a liquid membrane, $l_{optimum}$, is obtained at $\sigma \approx 1$ in eq 4, thereby yielding

Equation 2-10 $$l_{optimum} \cong z\sqrt{\frac{D_m RT}{|z_i|F\upsilon}}$$

Equation 10 implies that a stripping step at a slower scan rate allows for the use of a thicker membrane with a higher capacity. Moreover, the Q_{eq} value is proportional to the preconcentration factor, which exponentially depends on the overpotential at the PVC

membrane/sample solution interface (eq 8). Consequently, the overpotential must be controlled precisely for equilibrium preconcentration despite the complication due to the polarization of the PVC/POT/gold junction (eq 5). In contrast, neither the thickness of a thin-layer membrane nor the preconcentration potential affects the sensitivity of the stripping current response when the preconcentration time is short enough to achieve the diffusion-limited preconcentration.

2.4.5 Modeling a Preconcentration Step

A preconcentration step was modeled to confirm that the saturation of a stripping voltammetric response is due to the equilibrium preconcentration of perchlorate in the thin-layer liquid membrane. Our model demonstrates that even under a rotating electrode configuration, the current during a preconcentration step, *i(t)*, decays exponentially as given by (see Supporting Information)

Equation 2-11

$$i(t) = i_{\mathrm{l}} \exp\left(-\frac{i_{\mathrm{l}} t}{Q_{\mathrm{eq}}} \right)$$

where the initial condition is approximated as $i(0) = i_{\mathrm{l}}$ so that the transient transfer of perchlorate immediately after the potential step at $t = 0$ is neglected. The integration of the current response during the preconcentration step with a duration of t_{p} gives the ionic charge accumulated in the membrane, $Q(t_{\mathrm{p}})$, as

Equation 2-12

$$Q(t_{\mathrm{p}}) = Q_{\mathrm{eq}} \left[1 - \exp\left(-\frac{i_{\mathrm{l}}}{Q_{\mathrm{eq}}} t_{\mathrm{p}} \right) \right]$$

Equation 12 indicates that $Q(t_{\mathrm{p}})$ varies linearly with the analyte concentration in the sample solution, because $i_{\mathrm{l}}/Q_{\mathrm{eq}}$ is independent of the concentration (see below). Thus, the stripping

current response is also proportional to the analyte concentration when the response is proportional to $Q(t_p)$.

The aforementioned model was validated experimentally. The total charge that is obtainable during a stripping step, Q_s, is given by

Equation 2-13 $$Q_s = Q(t_p) + Q_{bg}$$

where Q_{bg} is the charge due to background processes such as interfacial charging during the stripping step and the transient perchlorate transfer at the initial stage of a preconcentration step. The plot of Q_s versus t_p obtained with 100 nM perchlorate fits well with eq 13 (the inset of Figure 5), thereby yielding Q_{eq} and i_l values as well as a Q_{bg} value of 1.5 ± 0.2 μC. The i_l value of 37 ± 9 nA thus obtained agrees with the value of 37 nA expected from eq 7 with c_0 = 100 nM. The Q_{eq} value of 1.95 ± 0.03 μC obtained from the fits corresponds to $Y = (1.43 \pm 0.02) \times 10^4$ in eq 9 with l = 0.72 μm, indicating that the equilibrium membrane ion concentration is higher than the sample ion concentration by 4 orders of magnitude. The preconcentration ratio corresponds to an overpotential, $\Delta^{m}_{w}\phi^{p} - \Delta^{m}_{w}\phi^{0'}_{ClO_4^-}$, of 0.25 V in eq 8. This overpotential agrees with the value expected from eq 6 with E_{app} = 0.95 V during the preconcentration step. This applied potential is very close to the anodic limit of a potential window at the PVC membrane/sample solution interface.

Importantly, eq 12 also predicts that the response time of hydrodynamic ion-transfer stripping voltammetry with a thin-layer liquid membrane is independent of the analyte concentration in the sample solution in contrast to traditional ion-selective potentiometry. The time constant of a preconcentration step as defined by Q_{eq}/i_l in eq 12 is given by a combination of eqs 7 and 9 as

Equation 2-14

$$\frac{Q_{eq}}{i_l} = \frac{lY}{0.62 D_w^{2/3} \omega^{1/2} \nu^{-1/6}}$$

This time constant is independent of the analyte concentration and dominates the response time of ion-transfer stripping voltammetry because a preconcentration step takes much longer than a stripping step. In potentiometry, the response time at a lower analyte concentration is prolonged up to a few hours even under a rotating electrode configuration.[61]

2.4.6 Limit of Detection (LOD) in Stripping Voltammetry

The LOD of perchlorate in deionized water was assessed for stripping voltammetry with a thin-layer PVC membrane under a rotating electrode configuration. The preconcentration time was optimized for the detection of 1-100 nMperchlorate, which is not only much lower than the current action limit (~246 nM) set by the EPA[8] but also comparable to or lower than the concentration range of trace perchlorate found in drinking water,[2] human and cow's milk,[3] and produce.[4]

A short preconcentration time of 30 s was enough to readily detect 10-100 nM perchlorate in deionized water (Figure 6a). Moreover, the stripping peak current was clearly observed with 1-10 nM perchlorate after 10 min equilibrium preconcentration (Figure 6b). In either concentration range, the backgroundsubtracted current response is linear to the sample ion concentration (the insets of the respective figures). The linearity confirms that the current response either after equilibrium or nonequilibrium preconcentration varies with $Q(t_p)$, which is proportional to the sample concentration (eqs 9 and 12). A LOD was determined from the linear

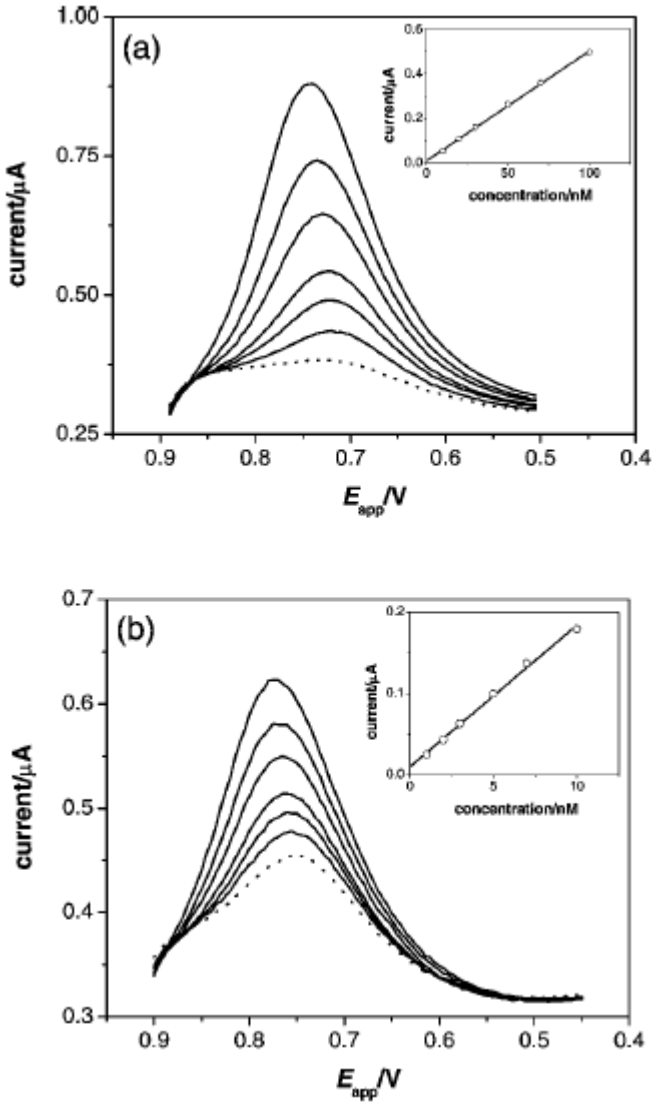

Figure 2-6. Stripping voltammograms of (a) 100, 70, 50, 30, 20, 10, and 0 nM and (b) 10, 7, 5, 3, 2, 1, and 0 nM perchlorate (from the top) in deionized water at 0.1 V/s. The insets show the plots of the background-subtracted peak current versus the perchlorate concentrations. The preconcentration time was (a) 30 s and (b) 10 min. The electrode was rotated at 4000 rpm.

relationship of the stripping peak current with 1-10 nM perchlorate using the IUPAC's uper limit approach,[62] thereby yielding a LOD of 0.5 ± 0.1 nM perchlorate at a confidence level of 95% (see Supporting Information). This LOD is comparable to the LODs of the most sensitive methods for detecting perchlorate, such as ion-chromatography coupled with a suppressed conductivity detector (0.55 nM)[12] or ESI-MS (0.20-0.25 nM).[15,16]

The LOD of the voltammetric perchlorate-selective electrode is ~36 times lower than the LOD of the potentiometric counterpart under a stationary condition.[22] A lower LOD may be obtained by potentiometry under a rotating electrode configuration.[61] Moreover, the equilibrium partition of perchlorate between the membrane and sample phases is governed by the Nernst equation in either voltammetric or potentiometric ISEs. Nevertheless, the stripping voltammetric approach is more sensitive in principle than the potentiometric approach, because the former requires a lower membrane ion concentration than the latter. The LOD of 0.5 nM perchlorate corresponds to a membrane perchlorate concentration of 7 μM in eq 8 with $Y = 1.43 \times 10^4$. This membrane ion concentration is much lower than the standard (~20 mM)[22] and lowest (>50 μM)[63] membrane concentrations of analyte ions required for potentiometric ISEs. The lower operational concentration of analyte ions in our voltammetric membranes is achieved within a shorter response time, thereby practically yielding a lower detection limit.

Although more work is needed, we speculate that the background response that resembles the stripping voltammogram of perchlorate (Figure 6b) is due to the perchlorate molecules contaminated in the POT film during its electrochemical deposition in the presence of 0.5 M $LiClO_4$. Unfortunately, the high concentration of $LiClO_4$ is required for the deposition of the stable POT film that is not easily soluble in THF during spin-coating of a PVC membrane. The

background response is independent of the concentration of the aqueous supporting electrolyte, Li_2SO_4, which is not a source of perchlorate contamination.

2.4.7 Stripping Analysis of Nanomolar Perchlorate in Drinking Water

Nanomolar perchlorate in tap water and commercial bottled water was detectable by stripping voltammetry with a thinlayer PVC membrane electrode. A stripping response was observed with 1-10 nM perchlorate spiked in a bottled water sample after 10 min equilibrium preconcentration (Figure 7). The background- subtracted peak current was linear to the aqueous perchlorate concentration, thereby yielding a LOD of 0.2 ± 0.1 nM (see Supporting Information). No significant response to an interfering species in bottled water was detected in the background stripping voltammogram, which is similar to that obtained with deionized water. The background peak response is not due to perchlorate contamination in bottled water because a nearly identical response was observed with the mixture of bottled water and deionized water (50:50 v/v).

In contrast to deionized and bottled water samples, tap water contains a low concentration of an interfering anion, which is detectable by ion-transfer stripping voltammetry but not by cyclic voltammetry. As the preconcentration time increased, the background current response increased and then leveled off after 10 min preconcentration (Figure 8). This current response was observed at more anodic potentials than the perchlorate response, indicating that the interfering ion is more lipophilic than perchlorate perchlorate. The plot of Q_s versus t_p fits well with eq 13, thereby yielding Q_{eq} = 1.0 μC, i_l = 3.4 nA, and Q_{bg} = 1.85 μC. The i_l value is 11 times smaller than the corresponding value of 37 nA for 100 nM perchlorate and is equivalent to c_0 = ~9 nM in eq 7 if the interfering ion has the same charge number and diffusion coefficient as

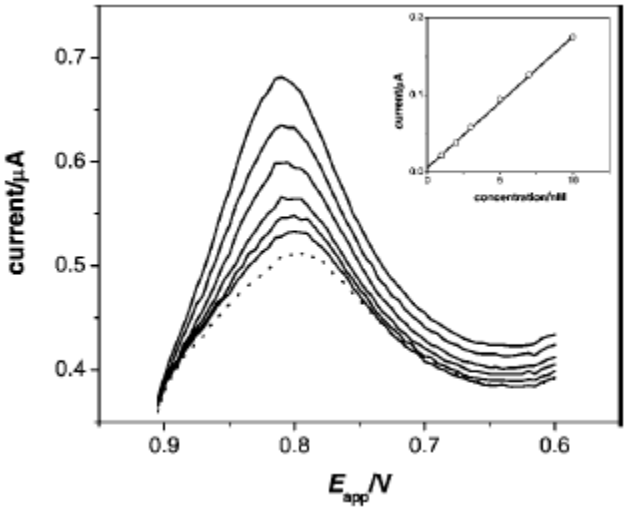

Figure 2-7. Stripping voltammograms of 10, 7, 5, 3, 2, 1, and 0 nM perchlorate (from the top) in commercial bottled water at 0.1 V/s. The inset shows the plot of the background-subtracted peak current versus the perchlorate concentrations. The preconcentration time was 10 min. The electrode was rotated at 4000 rpm.

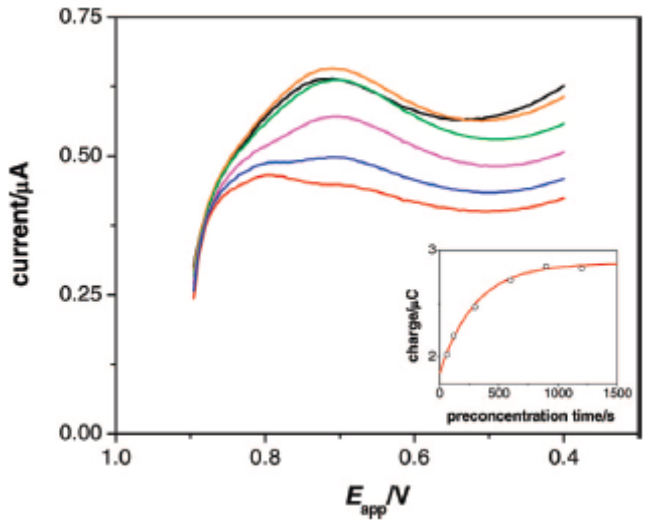

Figure 2-8. (a) Background stripping voltammograms at 0.1 V/s in tap water without perchlorate after a preconcentration step of 10 (red), 30 (blue), 60 (magenta), 120 (green), 300 (orange), and 600 (black) s. The inset shows the plot of Qs versus tp, where the O and the solid line represent experimental and theoretical (eq 13) values, respectively. The electrode was rotated at 4000 rpm.

perchlorate. Despite the apparently much lower concentration, the Q_{eq} value for the interfering ion is comparable to a value of 1.5 μC for 100 nM perchlorate. This result is ascribed to a larger *Y* value for the interfering ion as defined by eq 8, where the potential applied to the gold electrode during a preconcentration step corresponds to a larger overpotential for the more lipophilic interfering ion with a more negative formal ion-transfer potential. Importantly, the time constant of a preconcentration step, Q_{eq}/i_l, is smaller for perchlorate than for the interfering ion by an order of magnitude (40 and 300 s, respectively, at this applied potential) so that the equilibrium preconcentration of perchlorate is completed ~10 times faster than that of the interfering ion.

A stripping voltammetric response was measured with 1-10 nM perchlorate in tap water after 3 min preconcentration (Figure 9), which is long enough for perchlorate but too short for the interfering ion to achieve the equilibrium preconcentration. The current response to perchlorate was nearly as large as expected for saturation. The background-subtracted peak current response to perchlorate is linear to its concentration (the inset of Figure 9), thereby obtaining a LOD of 0.4 ± 0.2 nM (see Supporting Information). On the other hand, the current response to the interfering ion was significantly suppressed as expected for the short preconcentration time. This result demonstrates the advantage of ion-transfer stripping voltammetry in selectivity; the stripping current response based on the thermodynamically more favorable transfer of an interfering ion is not only dislocated with respect to the response to an analyte ion but also suppressed selectively by shortening the preconcentration time.

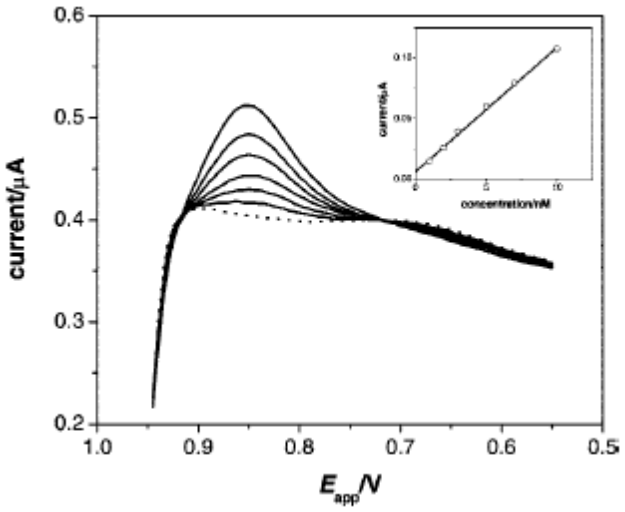

Figure 2-9. Stripping voltammograms of 10, 7, 5, 3, 2, 1, and 0 nM perchlorate (from the top) in tap water at 0.1 V/s. The inset shows the plot of the background-subtracted peak current versus the perchlorate concentrations. The preconcentration time was 3 min. The electrode was rotated at 4000 rpm.

2.5 CONCLUSIONS

A voltammetric ISE was developed for the stripping analysis of nanomolar perchlorate in drinking water samples. The detection limits of this ISE are lower than not only the current action limit set by the EPA but also the trace concentrations of perchlorate found in the drinking water. Moreover, the voltammetric perchlorate-selective electrode gives as low detection limits as the currently most sensitive methods for detecting perchlorate such as ion chromatography coupled with a suppressed conductivity detector or ESI-MS. At the same time, the voltammetric ISE is advantageous in cost, portability, and analysis time against these techniques, thereby rendering this electrochemical sensor potentially useful for the trace analysis of perchlorate in drinking water.

This work is the first to demonstrate the thin-layer behavior of a liquid membrane in ion-transfer stripping voltammetry. The detection limits of 0.2-0.5 nM perchlorate are lower than the lowest detection limits of several nanomolar obtained so far by ion-transfer stripping voltammetry with a thicker liquid membrane.[38,44] The subnanomolar detection limits, however, are rather moderate in comparison to the picomolar detection limits of anodic stripping voltammetry with a thin mercury electrode.[64] The moderate detection limits are due to the small overpotential of 0.25 V applied during the preconcentration step of perchlorate, which quickly reaches the equilibrium. In fact, this overpotential is smaller than the value of 0.3-0.4 V recommended for anodic stripping voltammetry.[28] This smaller overpotential is limited by the anodic potential window at the PVC membrane/sample solution despite the nearly highest lipophilicity of perchlorate in the Hofmeister series of inorganic anions.[65] Nevertheless, our

approach is still complementary or potentially alternative to anodic stripping voltammetry, which requires the amalgamation of an analyte as well as the use of a mercury electrode.[66]

A lower detection limit will be obtainable for more lipophilic ions or the ions that can be transferred into the membrane more preferentially by complexation with ionophores. The formal potential of these ion transfers is further from the limit of a potential window so that a larger overpotential is applied to achieve the diffusion-limited preconcentration for a longer duration. Another advantage of the diffusion-limited preconcentration is that it does not require the precise control of the applied potential at the PVC membrane/sample solution interface. The intrinsically limited redox capacity of the POT film causes the potential distribution across the various interfaces in the solid-supported double-polymer system, thereby complicating the precise control of the overpotential at the target interface.

In comparison to the potentiometric counterpart, ion-transfer stripping voltammetry with a thin-layer liquid membrane offers advantages in a detection limit, a response time, and selectivity. A lower detection limit or a shorter response time is obtained with the voltammetric approach, which requires the smaller amount of analyte ions in the membrane. The even smaller amount of an analyte ion in the membrane will be detectable voltammetrically by suppressing the background current response during a stripping step. The selective detection of perchlorate in tap water containing an unknown interfering ion demonstrates another important advantage that voltammetric ion selectivity is controlled by formal ion-transfer potentials not only thermodynamically as the different stripping peak potentials but also dynamically as the different times required for the equilibrium preconcentration. Potentiometric ion selectivity is determined only thermodynamically by the difference of formal ion-transfer potentials as the basis of a selectivity coefficient.[23]

ACKNOWLEDGEMENTS

This work was supported by a CAREER award from the National Science Foundation (Grant CHE-0645623). The authors thank Jidong Guo for preliminary experiments and Patrick J. Rodgers for careful reading of this manuscript.

SUPPORTING INFORMATION

Diffusion Problem at Liquid Membrane/Water Interfaces

The simulated CVs in the main text were obtained by solving the following diffusion problem. The diffusion of an analyte ion in the aqueous phase is expressed as

$$\frac{\partial c_{\mathrm{w}}(x,t)}{\partial t} = D_W\left[\frac{\partial^2 c_{\mathrm{w}}(x,t)}{\partial x^2}\right] \qquad (0 < x) \qquad \text{(S1)}$$

where $c_{\mathrm{w}}(x,t)$ is the local concentration of the transferring ion in the aqueous phase. The diffusion of the ion in the membrane phase is expressed as

$$\frac{\partial c_{\mathrm{m}}(x,t)}{\partial t} = D_m\left[\frac{\partial^2 c_{\mathrm{m}}(x,t)}{\partial x^2}\right] \qquad (-l < x < 0) \qquad \text{(S2)}$$

where $c_{\mathrm{m}}(x,t)$ is the local concentration of the ion in the membrane phase. The membrane phase represents only a PVC membrane because the distribution of perchlorate into the underlying POT film is negligible (see Results and Discussion).

The boundary condition at the membrane/water interface (x = 0) is given by

$$D_m\left[\frac{\partial c_m(x,t)}{\partial x}\right]_{x=0} = D_W\left[\frac{\partial c_W(x,t)}{\partial x}\right]_{x=0} = k_f c_W(0,t) - k_b c_m(0,t) \quad \text{(S3)}$$

where k_f and k_b are the first-order heterogeneous rate constants for the forward and reverse transfers in eq 1, respectively. The rate constants are given by Butler-Volmer-type relations as[S1, S2]

$$k_f = k^0 \exp\left[-\alpha z_i F\left(\Delta_W^m\phi - \Delta_W^m\phi^{0'}\right)/RT\right] \quad \text{(S4)}$$

$$k_b = k^0 \exp\left[(1-\alpha) z_i F\left(\Delta_W^m\phi - \Delta_W^m\phi^{0'}\right)/RT\right] \quad \text{(S5)}$$

where k^0 is the standard rate constant, α is the transfer coefficient. In cyclic voltammetry, the potential is swept linearly at a constant rate, v, from the initial potential, $\Delta_W^m\phi^{0'}$, and the sweep direction is reversed at the switching potential, $\Delta_W^m\phi_\lambda{}^{0'}$, maintaining the potential sweep rate. This triangle potential wave is expressed as[S3]

$$\Delta_W^m\phi = \Delta_W^m\phi_i + \frac{2\left(\Delta_W^m\phi_\lambda - \Delta_W^m\phi_i\right)}{\pi}\sin^{-1}\left\{\sin\left[\frac{\pi v t}{2\left(\Delta_W^m\phi_\lambda - \Delta_W^m\phi_i\right)}\right]\right\} \quad \text{(S6)}$$

Other boundary conditions are given by

$$D_m\left[\frac{\partial c_m(x,t)}{\partial x}\right]_{x=-l} = 0 \qquad \text{(membrane/solid support interface)} \quad \text{(S7)}$$

$$\lim_{x\to 0} c_W(x,0) = c_0 \qquad \text{(membrane/solid support interface)} \quad \text{(S8)}$$

Initial conditions are given by

$$c_W(x,0) = c_0 \quad \text{(S9)}$$

$$c_m(x,0) = 0 \quad \text{(S10)}$$

The current response based on the ion transfer, i, is obtained from the flux of the transferring ion at the membrane/sample solution interface as

$$i = z_i AFD_W \left[\frac{\partial c_W(x,t)}{\partial x} \right]_{x=0} \quad \text{(S11)}$$

Finite Element Simulation by COMSOL Multiphysics

The diffusion problem defined above was solved in a dimensionless form by using COMSOL Multiphysics. The example of the finite element simulation is attached. Dimensionless parameters are defined by

$$C_w(X, \tau) = c_w(x, t)/c_0 \quad \text{(S12)}$$

$$C_m(X, \tau) = c_m(x, t)/c_0 \quad \text{(S13)}$$

$$X = x/l \quad \text{(S14)}$$

$$\tau = D_w t/l^2 \quad \text{(S15)}$$

Diffusion processes (eqs S1 and S2) are expressed in the respective dimensionless forms as

$$\frac{\partial C_w(X,\tau)}{\partial \tau} = \gamma \left[\frac{\partial^2 C_w(X,\tau)}{\partial X^2} \right] \quad \text{(S16)}$$

$$\frac{\partial C_m(X,\tau)}{\partial \tau} = \left[\frac{\partial^2 C_m(X,\tau)}{\partial X^2} \right] \quad \text{(S17)}$$

with

$$\gamma = D_w/D_m \quad \text{(S18)}$$

The boundary condition at the liquid/liquid interface (eq S3) is expressed using the dimensionless parameters as

$$\gamma \left[\frac{\partial C_w(X,\tau)}{\partial X} \right]_{X=0} = K\theta^{(1-\alpha)} \left[\frac{C_m(0,\tau)}{\theta} - C_w(0,\tau) \right] \quad \text{(S19)}$$

$$\left[\frac{\partial C_m(X,\tau)}{\partial X} \right]_{X=0} = -\frac{K}{\theta^{\alpha}} \left[\theta C_w(0,\tau) - C_m(0,\tau) \right] \quad \text{(S20)}$$

with

$$K = k^0 l/D_w \tag{S21}$$

$$\theta = \exp\left[\frac{z_i F(\Delta_w^m \phi - \Delta_w^m \phi_i^{0'})}{RT}\right] \tag{S22}$$

K = 100 was used for the nernstian ion transfer. The triangle potential wave (eq S6) was given by

$$\theta = \theta_i^{1-(2/\pi)\sin^{-1}\{\sin[\pi\sigma\tau/2\ln(\theta_\lambda/\theta_i)]\}}\theta_\lambda^{(2/\pi)\sin^{-1}\{\sin[\pi\sigma\tau/2\ln(\theta_\lambda/\theta_i)]\}} \tag{S23}$$

with

$$\theta_i = \exp\left[\frac{z_i F(\Delta_w^m \phi_i - \Delta_w^m \phi_i^{0'})}{RT}\right] \tag{S24}$$

$$\theta_\lambda = \exp\left[\frac{z_i F(\Delta_w^m \phi_\lambda - \Delta_w^m \phi_i^{0'})}{RT}\right] \tag{S25}$$

$$\tau_\lambda = \frac{z_i F(\Delta_w^m \phi_\lambda - \Delta_w^m \phi_i)}{RT\sigma} \tag{S26}$$

where θ_i is the initial and final potentials in the dimensionless form, θ_λ is the dimensionless switching potential, and τ_λ is the dimensionless switching time. The other boundary conditions and the initial conditions are also given using the dimensionless parameters (see the attached example). The current was normalized with respect to the peak current on the forward scan, i_{pa}, thereby yielding

$$I = \frac{i}{i_{pa}} = \frac{[\partial C_w(0,\tau)/\partial X]}{[\partial C_w(0,\tau)/\partial X]_{pa}} \tag{S27}$$

where $[\partial C_w(0,\tau)/\partial X]_{pa}$ is the interfacial gradient of a dimensionless concentration at the anodic peak potential.

Determination of the Diffusion Coefficient of Perchlorate in the PVC Membrane

The diffusion coefficient of perchlorate in the PVC membrane was determined from the CVs of perchlorate transfer using the 3 μm-thick PVC membrane drop-cast on the POT-modified gold electrode. The preparation of the drop-cast PVC membrane electrode was reported elsewhere.[S4] As the scan rate decreased from 1 V/s to 0.1 V/s (red lines in Figure 10a and b, respectively), the ratio of the cathodic peak current with respect to the anodic one increased, indicating that the perchlorate diffusion in the drop-cast membrane is hindered by the underlying POT-modified gold electrode at the slower scan rate. The CV at 0.1 V/s fits best with the simulated nernstian CV with σ = 7, D_w = 1.7 ×10^{-5} cm^2/s, and $\partial\Delta_w^{PVC}\phi / \partial E_{app}$ = 0.85. Eq 15 with σ = 7, ν = 0.1 V/s, and l = 3 μm gives D_m = 5.0 × 10^{-8} cm^2/s, which is ~340 times smaller than the D_w value.

We speculate that the deviation of the experimental CV at 0.1 V/s from the simulated CV is due to the presence of a mixed layer, which was formed at the interface between the PVC and POT phases during the drop cast. In fact, the experimental and simulated CVs at either 1 or 0.1 V/s fit very well with the spin-coated PVC membrane (Figures 3a and b), suggesting that the quick evaporation of THF during the spin coating avoids the dissolution of the POT film and concomitantly the formation of the mixed layer. Moreover, a much better fit was obtained for the CV at 1 V/s even with the drop-cast PVC membrane, where perchlorate cannot diffuse into the mixed layer during the faster potential sweep.

The nernstian transfer of perchlorate is demonstrated by the convoluted transform, $I(t)$, of the CV at 1 V/s. The pair of the nearly overlapping sigmoidal waves in the $I(t)$ versus E_{app} plot indicates that the CV is controlled by the semi-infinite linear diffusion of perchlorate both in the aqueous and membrane phases (blue line in Figure 10a).[S4] The dependence of the convoluted

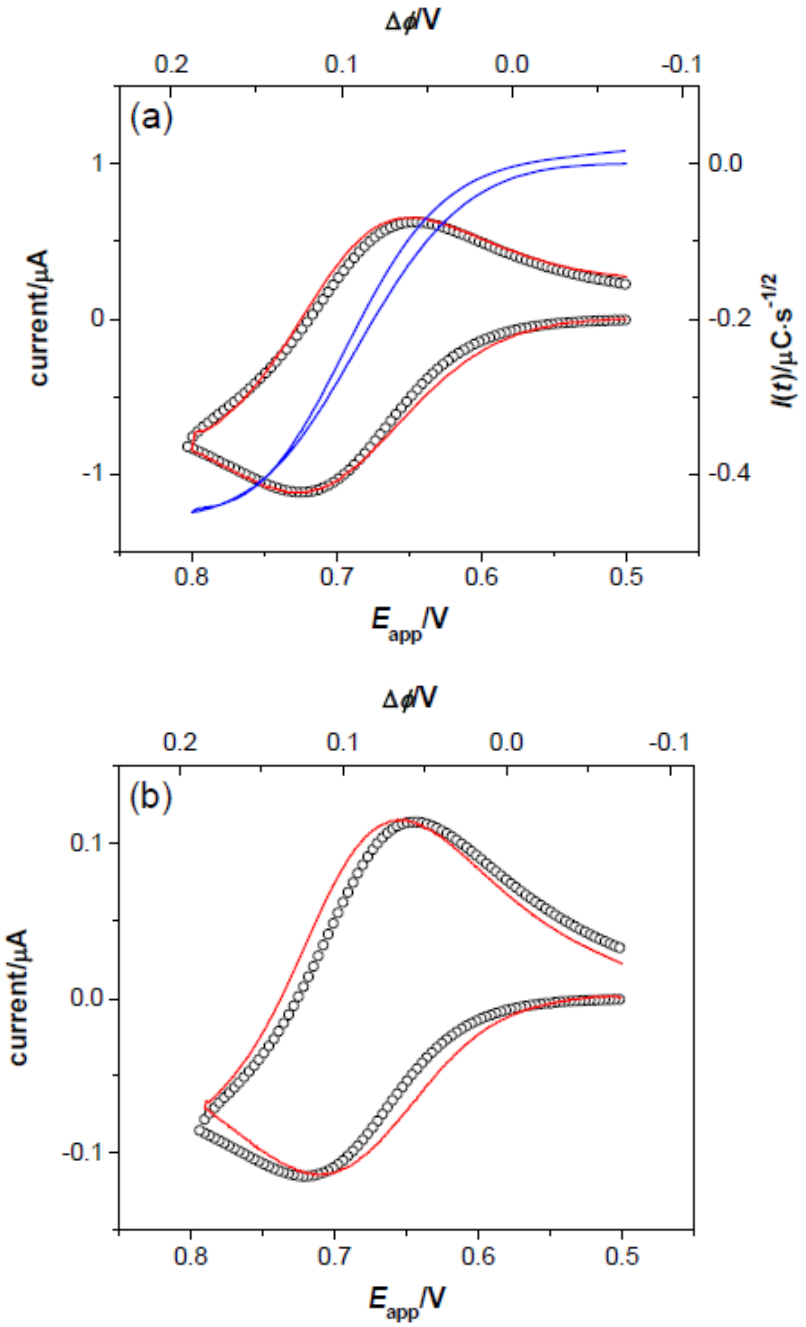

Figure 2-10. Experimental (red line) and simulated (circles) CVs of perchlorate with the 3 μm-thick PVC membrane drop-cast on the POT-modified gold electrode at (a) 1 and (b) 0.1 V/s with 20 and 60 μM ClO_4^-, respectively. The blue line represents the convoluted form of the CV.

form on E_{app} corresponds to $\partial\Delta_w^{PVC}\phi/\partial E_{app}$ = 0.71. The limiting value in the convoluted form gives D_w = 1.7 ×10^{-5} cm^2/s, which is close to a literature value of 1.8 × 10^{-5} cm^2/s.[S5] These parameters agree with D_w = 1.9 ×10^{-5} cm^2/s and $\partial\Delta_w^{PVC}\phi/\partial E_{app}$ = 0.82 as determined by the numerical simulation.

Derivation of Eq 11

The exponential decay of the current response during a preconcentration step (eq 11) is demonstrated as follows. Under a rotating electrode configuration, the current response limited by the mass transfer of the aqueous perchlorate, $i(t)$, is directly related to $c_w(0,t)$ using eq 7, thereby yielding

$$i(t) = 0.62 z_i F A D_w^{2/3} \omega^{1/2} \nu^{-1/6} [c_0 - c_w(0,t)] \quad \text{(S29)}$$

A combination of eqs 7 and S29 results in

$$c_w(0,t) = c_0 \frac{i_l - i(t)}{i_l} \quad \text{(S30)}$$

On the other hand, the membrane concentration of an analyte ion is given by integrating the current as

$$c_m(t) = \frac{\int_0^t i(\tau) d\tau}{z_i F A l} \quad \text{(S31)}$$

A combination of eq 19 with eqs S30 and S31 gives

$$\frac{i_l \int_0^t i(\tau) d\tau}{z_i F A l c_0 [i_l - i(t)]} = Y \quad \text{(S32)}$$

Using eq 9, eq S32 can be simplified to

$$\frac{\int_0^t i(\tau)d\tau}{Q_{eq}} = \frac{i_l - i(t)}{i_l} \quad \text{(S33)}$$

Eq S33 can be solved for $i(t)$ analytically using the Laplace transformationS6 to obtain eq 11, where the initial condition of $i(0) = i_l$ was assumed. It implies that the current decays to i_l immediately after the potential step at $t = 0$.

Limit of Detection (LOD) Determined from a Calibration Plot

A LOD was determined using the Upper Limit Approach developed by the IUPAC.[S7] The calibration curves in the insets of Figures 6b, 7, and 9 were fitted with the following equation

$$i_{pa} = q_0 + q_1 c_0 \quad \text{(S34)}$$

yielding q_0 and q_1 values as well as the mean square about the regression, s_y^2. Eq 37 in ref. S8 was used to determine whether the intercept is significantly different from 0 at the 95 % confidence level. If it is, a LOD was obtained at this confidence level using eq 31 in ref. S8. Otherwise, a LOD was determined at the same confidence level using eq 36a.

Supporting Info References

(S1) Samec, Z.; Homolka, D.; Marecek, V. *J. Electroanal. Chem.* **1982**, *135*, 265–283.

(S2) Samec, Z. *Pure Appl. Chem.* **2004**, *76*, 2147–2180.

(S3) Weisstein, E. W. "Triangle Wave." From MathWorld--A Wolfram Web Resource (http://mathworld.wolfram.com/TriangleWave.html).

(S4) Guo, J.; Amemiya, S. *Anal. Chem.* **2006**, *78*, 6893–6902.

(S5) Wilke, S.; Zerihun, T. *J. Electroanal. Chem.* **2001**, *515*, 52–60.

(S6) Bard, A. J.; Faulkner, L. R. *Electrochemical Methods: Fundamentals and Applications*, 2nd ed.; John Wiley & Sons: New York, 2001, pp 770–772.

(S7) Mocak, J.; Bond, A. M.; Mitchell, S.; Scollary, G. *Pure Appl. Chem.* **1997**, *69*, 297–328.

COMSOL Model

A copy of the COMSOL model is available free of charge in the Supporting Information via the Internet at http://pubs.acs.org/doi/suppl/10.1021/ac8008687.

REFERENCES

(1) *Health Implications of Perchlorate Ingestion*; National Academies Press: Washington, DC, 2005.

(2) Motzer, W. E. *Environ. Forensics* **2001**, *2*, 301–311.

(3) Kirk, A. B.; Smith, E. E.; Tian, K.; Anderson, T. A.; Dasgupta, P. K. *Environ. Sci. Technol.* **2003**, *37*, 4979–4981.

(4) Jackson, W. A.; Joseph, P.; Laxman, P.; Tan, K.; Smith, P. N.; Yu, L.; Anderson, T. A. *J. Agric. Food Chem.* **2005**, *53*, 369–373.

(5) Kirk, A. B. *Anal. Chim. Acta* **2006**, *567*, 4–12.

(6) Dohan, O.; De la Vieja, A.; Paroder, V.; Riedel, C.; Artani, M.; Reed, M.; Ginter, C. S.; Carrasco, N. *Endocr. Rev.* **2003**, *24*, 48–77.

(7) Dohan, O.; Portulano, C.; Basquin, C.; Reyna-Neyra, A.; Amzel, L. M.; Carrasco, N. *Proc. Natl. Acad. Sci. U.S.A.* **2007**, *104*, 20250–20255.

(8) U.S. Environmental Protection Agency. http://yosemite.epa.gov/opa/admpress.nsf/b1ab9f485b098972852562e7004dc686/c1a57d2077c4bfda85256fac005b8b32!opendocument, **2005**.

(9) Urbansky, E. T. *Crit. Rev. Anal. Chem.* **2000**, *30*, 311–343.

(10) Hautman, D. P.; Munch, D.; Eaton, A. D.; Haghani, A. W. http://www.epa.gov/safewater/methods/sourcalt.html, **1999**.

(11) Wagner, H. P.; Pepich, B. V.; Pohl, C.; Later, D.; Joyce, R.; Srinivasan, K.; BeBorba, B.; Thomas, D.; Woodruff, A.; Munch, D. J. , EPA-815-R-805-009, http://www.epa.gov/safewater/ methods/sourcalt.html, **2005**.

(12) Wagner, H. P.; Pepich, B. V.; Pohl, C.; Later, D.; Srinivasan, K.; Lin, R.; DeBorba, B.; Munch, D. J. *J. Chromatogr., A* **2007**, *1155*, 15–21.

(13) Wendelken, S. C.; Munch, D. J.; Pepich, B. V.; Later, D. W.; Pohl, C. A. , EPA-815-R-805-007, http://www.epa.gov/safewater/methods/sourcalt.html, **2005**.

(14) Hedrick, E.; Behymer, T.; Slingsby, R.; Munch, D. EPA/600/R-605/049, http://www.epa.gov/nerlcwww/ordmeth.htm, **2005**.

(15) Martinelango, P. K.; Anderson, J. L.; Dasgupta, P. K.; Armstrong, D. W.; Al-Horr, R. S.; Slingsby, R. W. *Anal. Chem.* **2005**, *77*, 4829–4835.

(16) Martinelango, P. K.; Dasgupta, P. K. *Anal. Chem.* **2007**, *79*, 7198–7200.

(17) Lang, G. G.; Horanyi, G. *J. Electroanal. Chem.* **2003**, *552*, 197–211.

(18) Wu, J. C.; Mullett, W. M.; Pawliszyn, J. *Anal. Chem.* **2002**, *74*, 4855–4859.

(19) Bakker, E.; Pretsch, E. *TrAC, Trends Anal. Chem.* **2005**, *24*, 199–207.

(20) Sokalski, T.; Ceresa, A.; Zwickl, T.; Pretsch, E. *J. Am. Chem. Soc.* **1997**, *119*, 11347–11348.

(21) Szigeti, Z.; Vigassy, T.; Bakker, E.; Pretsch, E. *Electroanalysis* **2006**, *18*, 1254–1265.

(22) Malon, A.; Radu, A.; Qin, W.; Qin, Y.; Ceresa, A.; Maj-Zurawska, M.; Bakker, E.; Pretsch, E. *Anal. Chem.* **2003**, *75*, 3865–3871.

(23) Amemiya, S. In *Handbook of Electrochemistry*; Zoski, C. G. , Ed.; Elsevier: New York, 2007; pp 261-294.

(24) Shvarev, A.; Bakker, E. *Anal. Chem.* **2003**, *75*, 4541–4550.

(25) Ceresa, A.; Radu, A.; Peper, S.; Bakker, E.; Pretsch, E. *Anal. Chem.* **2002**, *74*, 4027–4036.

(26) Guo, J.; Amemiya, S. *Anal. Chem.* **2006**, *78*, 6893–6902.

(27) Samec, Z.; Samcova´, E.; Girault, H. H. *Talanta* **2004**, *63*, 21–32.

(28) Wang, J. *Stripping Analysis: Principles, Instrumentation, and Applications*; VCH: Deerfield Beach, FL, 1985.

(29) Guo, J.; Yuan, Y.; Amemiya, S. *Anal. Chem.* **2005**, *77*, 5711–5719.

(30) Marecek, V.; Samec, Z. *Anal. Lett.* **1981**, *14*, 1241–1253.

(31) Marecek, V.; Samec, Z. *Anal. Chim. Acta* **1982**, *141*, 65–72.

(32) Marecek, V.; Samec, Z. *Anal. Chim. Acta* **1983**, *151*, 265–269.

(33) Homolka, D.; Marecek, V.; Samec, Z.; Base, K.; Wendt, H. *J. Electroanal. Chem.* **1984**, *163*, 159–170.

(34) Ohkouchi, T.; Kakutani, T.; Osakai, T.; Senda, M. *Anal. Sci.* **1991**, *7*, 371–376.

(35) Huang, B.; Yu, B.; Li, P.; Jiang, M.; Bi, Y.; Wu, S. *Anal. Chim. Acta* **1995**, *312*, 329–335.

(36) Yu, B. Z.; Huang, B.; Li, P. B. *Microchem. J.* **1995**, *52*, 10–21.

(37) Sun, L.; Weber, S. G. *Polym. Mater. Sci. Eng.* **1997**, *76*, 614–615.

(38) Katano, H.; Senda, M. *Anal. Sci.* **1998**, *14*, 63–65.

(39) Lee, H. J.; Beriet, C.; Girault, H. H. *Anal. Sci.* **1998**, *14*, 71–77.

(40) Senda, M.; Katano, H.; Yamada, M. *J. Electroanal. Chem.* **1999**, *468*, 34–41.

(41) Katano, H.; Senda, M. *J. Electroanal. Chem.* **2001**, *496*, 103–109.

(42) Senda, M.; Katano, H.; Kubota, Y. *Collect. Czech. Chem. Commun.* **2001**, *66*, 445–455.

(43) Katano, H.; Senda, M. *Anal. Sci.* **2001**, *17*, i337–i340.

(44) Sherburn, A.; Arrigan, D. W. M.; Dryfe, R. A. W.; Boag, N. M. *Electroanalysis* **2004**, *16*, 1227–1231.

(45) Fujii, K.; Tanibuchi, S.; Kihara, S. *Anal. Sci.* **2005**, *21*, 1415–1420.

(46) Donten, M.; Stojek, Z.; Kublik, Z. *J. Electroanal. Chem.* **1984**, *163*, 11–21.

(47) Nazarov, B. F.; Larionova, E. V.; Stromberg, A. G.; Antipenko, I. S. *Electrochem. Commun.* **2007**, *9*, 1936–1944.

(48) Guo, J.; Amemiya, S. *Anal. Chem.* **2005**, *77*, 2147–2156.

(49) Rodgers, P. J.; Amemiya, S. *Anal. Chem.* **2007**, *79*, 9276–9285.

(50) Samec, Z.; Homolka, D.; Marecek, V. *J. Electroanal. Chem.* **1982**, *135*, 265–283.

(51) Langmaier, J.; Stejskalova, K.; Samec, Z. *J. Electroanal. Chem.* **2002**, *521*, 81–86.

(52) Copeland, T. R.; Skogerboe, R. K. *Anal. Chem.* **1974**, *46*, 1257A–1268A

(53) Bard, A. J.; Faulkner, L. R. *Electrochemical Methods: Fundamentals and Applications*, 2nd ed.; John Wiley and Sons: New York, 2001; pp 458-464.

(54) Vries, E. T. D.; Dalen, E. V. *J. Electroanal. Chem.* **1964**, *8*, 366–377.

(55) Shi, C.; Anson, F. C. *Anal. Chem.* **1998**, *70*, 3114–3118.

(56) Langmaier, J.; Olsak, J.; Samcova, E.; Samec, Z.; Trojanek, A. *Electroanalysis* **2006**, *18*, 1329–1338.

(57) Bard, A. J.; Faulkner, L. R. *Electrochemical Methods: Fundamentals and Applications*, 2nd ed.; John Wiley and Sons: New York, 2001; p 339.

(58) Ye, Q. S.; Meyerhoff, M. E. *Anal. Chem.* **2001**, *73*, 332–336.

(59) Galceran, J.; Companys, E.; Puy, J.; Cecilia, J.; Garces, J. L. *J. Electroanal. Chem.* **2004**, *566*, 95–109.

(60) Huidobro, C.; Companys, E.; Puy, J.; Galceran, J.; Pinheiro, J. P. *J. Electroanal. Chem.* **2007**, *606*, 134–140.

(61) Vigassy, T.; Gyurcsanyi, R. E.; Pretsch, E. *Electroanalysis* **2003**, *15*, 1270–1275.

(62) Mocak, J.; Bond, A. M.; Mitchell, S.; Scollary, G. *Pure Appl. Chem.* **1997**, *69*, 297–328.

(63) Ceresa, A.; Sokalski, T.; Pretsch, E. *J. Electroanal. Chem.* **2001**, *501*, 70–76.

(64) Wang, J. Electrochemical Preconcentration. In *Laboratory Techniques in Electroanalytical Chemistry*, 2nd ed.; Kissinger, P. T., Heineman, W. R. , Eds.; Marcel Dekker: New York, 1996; pp 719-737.

(65) Wegmann, D.; Weiss, H.; Ammann, D.; Morf, W. E.; Pretsch, E.; Sugahara, K.; Simon, W. *Mikrochim. Acta* **1984**, *3*, 1–16.

(66) Economou, A.; Fielden, P. R. *Analyst* **2003**, *128*, 205–212.

3.0 SUBNANOMOLAR ION DETECTION BY STRIPPING VOLTTAMETRY WITH SOLID-SUPPORTED THIN LIQUID MEMBRANE

This work has been published as Y. Kim, P. J. Rodgers, R. Ishimatsu, and S. Amemiya, *Anal. Chem.*, **2009**, *81*, 7262-7270.

3.1 INTRODUCTION

Dynamic ion transfer across the interface between two immiscible electrolyte solutions, i.e., ITIES, enables highly sensitive stripping voltammetry.[1] In comparison to traditional stripping voltammetry,[2,3] ion-transfer stripping voltammetry at the liquid/liquid interface is attractive for trace analysis of redox-inactive ions in environmental, biological, and biomedical samples. High sensitivity of this stripping method originates from preconcentration of an aqueous analyte ion into a water-immiscible organic phase, which is driven by external control of the phase boundary potential at the interface.[1,4] The preconcentration step is followed voltammetrically by reverse extraction of the ion from the organic phase into the aqueous phase to yield a stripping ionic current with enhanced sensitivity.

During the past decade, a limit of detection (LOD) of iontransfer stripping voltammetry has been lowered to nanomolar levels while micromolar limits were originally reported for

various ions including acetylcholine,[5] tetraethylammonium,[6] alkaline earth cations,[7] and protonated organic amines[8] by employing fluid organic phases. The improved sensitivity is mainly due to enhanced mass transfer of an analyte ion in the aqueous sample phase, which allows for more efficient preconcentration. Several to tens of nanomolar concentrations of Cd^{2+},[4] Zn^{2+},[4] Pb^{2+},[4,9] Hg^{2+},[9] and dodecylsulfonate[10] are detectable by rotating a plasticized poly(vinyl chloride) (PVC) membrane as a robust organic phase to hydrodynamically accelerate preconcentration of the analytes. Interestingly, nanomolar LODs were also obtained for electrically neutral surfactants, which were preconcentrated as charged complexes with aqueous cations in the membrane phase.[10-12] A plasticized PVC membrane was also integrated into a flow cell to detect 2 nM Ag^{+} by square-wave stripping voltammetry.[13] Alternatively, radial diffusion of aqueous analyte ions to a micrometer-sized interface[14] or an array of microinterfaces[15] was utilized for preconcentration of nanomolar heparin[16] or β-blocker propranolol,[17] respectively.

Recently, we applied a submicrometer-thick PVC membrane for stripping analysis of nanomolar perchlorate in various drinking waters.[18] The thin PVC membrane was supported by a Au electrode modified with an undoped poly(3-octhylthiophene) (POT) film, which was oxidized to drive anion transfer into the PVC membrane (Figure 1a).[18,19] An analyte ion is not only completely trapped in the solid-supported membrane during a preconcentration step but also exclusively stripped from the thinlayer membrane to maximize a stripping current response. LODs of ~0.5 nM perchlorate thus obtained are much lower than the interim health advisory level of 15 ppb (~150 nM) perchlorate in drinking water set by the U.S. Environmental Protection Agency.[20] These lowest LODs reported so far for ion-transfer stripping voltammetry, however, are an order of magnitude higher than subnanomolar LODs in the range of 10^{-10}-10^{-11} M as obtained by traditional anodic stripping voltammetry with a thin mercury film electrode.[3]

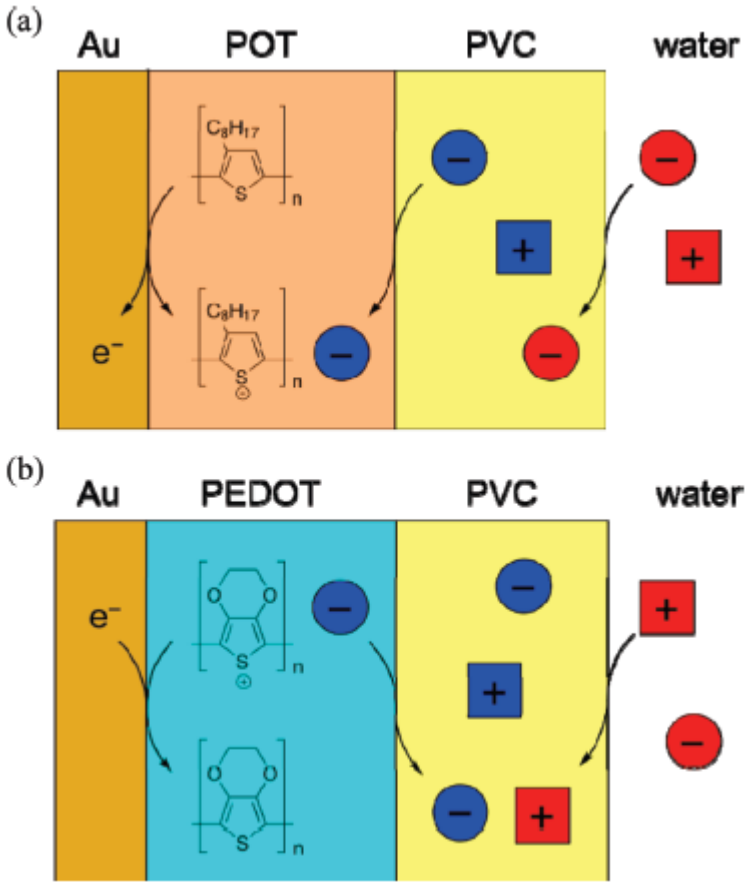

Figure 3-1. Scheme of (a) anion and (b) cation detection by iontransfer stripping voltammetry with thin PVC membranes coated on POT- and PEDOT-modified Au electrodes, respectively. Red circles and squares represent aqueous anionic and cationic analytes, respectively. Blue circles and squares correspond to organic anions and cations in the membrane phase, respectively.

Moreover, preconcentration of cationic analytes into the membrane phase requires reduction of an intermediate conducting-polymer layer while a POT film is not readily reduced or stable in an oxidized form, which is discharged to a reduced form under an open circuit condition.[19]

In this paper, we achieve subnanomolar LODs for both cationic and anionic analytes by ion-transfer stripping voltammetry with solid-supported thin polymeric membranes. These lower LODs represent the first experimental confirmation of a theoretical prediction that a more lipophilic analyte ion gives a lower LOD for stripping voltammetry with a solid-supported thin polymeric membrane.[18] Importantly, lipophilicity of either a cation or an anion is generally quantified by a preconcentration factor, *Y*,[18] (also known as the apparent ion partition coefficient[21]) to dictate an LOD as demonstrated in proof-of-concept experiments. A subnanomolar LOD of 80 nM tetrapropylammonium (TPA) is compared with a LOD of less lipophilic tetraethylammonium (TEA). Importantly, the voltammetric detection of cationic analytes is enabled by newly introducing an oxidatively doped poly(3,4-ethylenedioxythiophene) (PEDOT) film, which is reduced to preconcentrate cations in the PVC membrane (Figure 1b). This conducting polymer has a very high stability in the oxidized form and undergoes a facile redox reaction.[22,23] A practical significance of the theoretical prediction is demonstrated for trace analysis of a lipophilic inorganic anion, hexafluoroarsenate, which is known as an arsenical biocide[24,25] and was recently found in waste water.[26,27] An LOD of 90 nM hexafluoroarsenate as obtained with a PVC/POT-modified Au electrode is lower than that of less lipophilic perchlorate and compared to a LOD of hexafluoroarsenate by inductively coupled plasma mass spectrometry with anionexchange chromatography. Finally, the voltammetric anion- and cation-selective electrodes are characterized by electrochemical impedance spectroscopy (EIS). While both PVC/POT- and PVC/PEDOT-modified electrodes have been used for ion-selective

potentiometry,[28] the solid-supported PVC membranes for iontransfer stripping voltammetry must be not only thinner for exhaustive ion stripping[18] but also more conductive for avoiding a significant Ohmic potential drop in the membranes,[19] which is confirmed by EIS.

3.2 THEORY

Here we summarize theories of ion-transfer stripping voltammetry with a solid-supported thin polymeric membrane to explain how a more lipophilic ion gives a lower LOD. The proof of the following equations is given in our previous work.[18] Interestingly, the LOD based on dynamic ion transfer at the liquid/liquid interface is ultimately dictated by equilibrium partitioning of an analyte ion with charge z_i, i^{zi}, between the bulk aqueous and membrane phases

Equation 3-1 $$i^{z_i}(water) = i^{z_i}(membrane)$$

When an aqueous ion is preconcentrated into the solid-supported thin membrane with a small volume, equilibrium partitioning of the analyte ion is eventually achieved to limit a membrane concentration of the analyte ion. The equilibrium membrane concentration, c_{PVC}, with respect to the sample concentration, c_w, is defined in general for either a cation or an anion by a preconcentration factor, Y,[18] (also known as the apparent ion partition coefficient[21]) based on the Nernst equation as

Equation 3-2 $$Y = \frac{c_{PVC}}{c_W} = \exp\left[\frac{z_i F\left(\Delta_W^{PVC}\phi - \Delta_W^{PVC}\phi_i^{0'}\right)}{RT}\right]$$

where z_i is the charge of the analyte ion, F is Faraday's constant, $\Delta_W^{PVC}\phi$ is the Galvanic potential difference between the aqueous and PVC membrane phases, and $\Delta_W^{PVC}\phi_i^{0'}$ is the formal potential of the analyte ion. Since the amplitude of a stripping current response varies with the membrane

concentration, higher sensitivity and, subsequently, a lower LOD are expected for a more lipophilic ion with larger *Y*. In practice, the same potential near a negative (or positive) side of a potential window at the liquid/liquid interface is applied for cations (or anions) to result in a larger potential difference, $\Delta_W^{PVC}\phi - \Delta_W^{PVC}\phi_i^{0'}$, for a more lipophilic cation (or anion) with a more positive (or negative) formal potential,[21] thereby yielding a larger preconcentration factor.

Noticeably, eq 2 is valid not only for simple ion transfer but also for ion transfer facilitated by ionophores, where a formal potential depends on ion lipophilicity and stability of ion-ionophore complexes.[29] Nevertheless, this work is focused on simple ion transfer. Stripping voltammetry based on facilitated ion extraction at a solid-supported thin polymeric membrane requires greater understanding of mass transfers of ionophores and ion-ionophore complexes in the membrane.

A time-dependent preconcentration process was modeled to quantitatively demonstrate that a lower LOD based on equilibrium preconcentration of a more lipophilic ion requires longer preconcentration. The total charge of preconcentrated analyte ions, $Q(t_p)$, depends on preconcentration time, t_p, as given by[18]

Equation 3-3
$$Q(t_p) = Q_{eq}\left[1 - \exp\left(-\frac{i_l}{Q_{eq}}t_p\right)\right]$$

with

Equation 3-4
$$Q_{eq} = z_i FAlc_{PVC}$$

where Q_{eq} is the total charge at an equilibrium, A is an effective area of the PVC membrane/water interface, and l is an effective membrane thickness. Since the electrode is rotated during a preconcentration step (see Experimental Section), the limiting current, i_l, is given by the Levich equation as[30]

Equation 3-5

$$i_l = 0.62 z_i F A D_W^{2/3} \omega^{1/2} \nu^{-1/6} c_W$$

where D_w is a diffusion coefficient of the ion in the aqueous phase, ω is the angular frequency of electrode rotation, and ν is the kinematic viscosity. The time constant, Q_{eq}/i_l, in eq 3 is given by a combination of eqs 4 and 5 as

Equation 3-6

$$\frac{Q_{eq}}{i_l} = \frac{lY}{0.62 D_W^{2/3} \omega^{1/2} \nu^{-1/6}}$$

Equation 6 confirms that equilibrium partitioning of a more lipophilic ion with a larger preconcentration factor (see eq 2) requires longer preconcentration.

In the following, the aforementioned theoretical predictions are confirmed experimentally for cationic analytes, TEA and TPA, with different lipophilicities, which result in different time courses toward equilibrium partitioning of the respective ions within a practical preconcentration time (<1 h). The theoretical predictions are also tested for hexafluoroarsenate, a lipophilic anion with analytical importance. Overall, a trend of a lower LOD for an ion with larger Y is reported for the total of four cations and anions as summarized in Table 1.

3.3 EXPERIMENTAL SECTION

3.3.1 Chemicals

Tetradodecylammonium (TDDA) bromide, 3-octylthiophene, 3,4-ethylenedioxythiophene, tetrapropylammonium chloride, lithium sulfate monohydrate, and lithium hexafluoroarsenate (V)

Table 3-1. Comparison of Lipophilicity, *Y*, and LOD of Cationic and Anionic Analytes

	TPA	TEA	hexafluoroarsenate	perchlorate
Y	1.6×10^{5}	1.0×10^{4}	1.7×10^{5}	1.4×10^{4}
LOD/M	8×10^{-11}	4×10^{-10}	9×10^{-11}	5×10^{-10}

[a] Data from ref 18.

were obtained from Aldrich (Milwaukee, WI). Poly(vinyl chloride) (PVC, high molecular weight), tetraethylammonium chloride, and 2-nitrophenyl octyl ether were from Fluka (Milwaukee, WI). Potassium tetrakis(pentafluorophenyl)borate (TFAB) was from Boulder Scientific Company (Mead, CO). All reagents were used as received. The TFAB salt of TDDA was prepared as reported elsewhere.[19]

3.3.2 Electrode Modification

A 5 mm diameter Au disk attached to a rotating disk electrode tip (Pine Research Instrumentation, Raleigh, NC) was modified with a conducting polymer film and then with a PVC membrane. Preparation of a PVC/POT-modified Au electrode was reported elsewhere.[18] A PVC/PEDOT-modified Au electrode was prepared as follows.

A PEDOT film was deposited on a polished and cleaned Au electrode[18] with 5 mm diameter by cyclic voltammetry using a three-electrode cell with a Ag/Ag^+ reference electrode (CH Instruments) and a Pt-wire counter electrode. The film deposition was conducted in an acetonitrile solution containing 0.01 M 3,4-ethylenedioxythiophene and 0.01 M TDDATFAB by cycling the potential between -1.0 and 1.4 at 0.1 V/s 3 times using a computer-controlled CHI 600a electrochemical workstation (CH Instruments). The final potential was set to 0.5 V to oxidatively dope a PEDOT film with TFAB. The modified Au electrode was soaked in acetonitrile for 30 min and washed with THF for 1 min to remove soluble fractions of the PEDOT film. The remaining PEDOT film is not readily soluble in THF and can be spin-coated with a PVC membrane from a THF solution of membrane components.

A PVC membrane was spin-coated on a Au disk modified with a PEDOT film from a membrane cocktail with the composition of 4 mg of PVC, 16 mg of 2-nitrophenyl octyl ether,

and 2.2 mg of TDDATFAB in 1 mL of THF. A volume of 8 μL of the THF solution of the membrane cocktail was injected onto the PEDOT-modified Au disk rotating at 300 rpm in a spin-coating device (model SCSG3-8, Cookson Electronics, Providence, RI). The slow rotation resulted in a relatively thick PVC membrane with ~3 μm thickness, which was required for a good coverage of a PEDOT film. The modified Au disk (after spinning for 30 s) was removed from the spin coater and dried in the air for >30 min. A membrane cocktail with the same composition was employed to spin-coat a ~0.7 μm-thick PVC membrane on a POT-modified Au electrode rotating at 1500 rpm.[18] An effective thickness of a PVC membrane spin-coated on either PEDOT- or POT-modified Au electrode was determined by ion-transfer cyclic voltammetry as reported elsewhere.[18]

3.3.3 Voltammetric Measurements

Cyclic voltammetry and stripping voltammetry were performed by employing a CHI 900 electrochemical workstation (CH Instruments). A three-electrode arrangement with a Ag/AgCl reference electrode (CH Instruments) and a Pt-wire counter electrode was employed. Electrochemical cells were as follows:

Ag|AgCl|KCl (3 M)||xM TEACl or TPACl

in 0.01 M Li_2SO_4(aq)|PVC membrane|PEDOT|Au (cell 1)

Ag|AgCl|KCl (3 M)||yM $LiAsF_6$ in 0.01 M Li_2SO_4(aq)|PVC membrane|POT|Au (cell 2)

The analyte concentrations are given in the Results and Discussion. Aqueous sample solutions were prepared with 18.3 MΩ cm deionized water (Nanopure, Barnstead, Dubuque, IA). The current carried by a positive charge from the aqueous phase to the PVC membrane is defined to

be positive. All electrochemical experiments were performed at 22 ± 3 °C. A piece of Teflon tube[18,19] was put on a membrane-modified Au electrode tip for cyclic voltammetry to obtain a disk-shaped PVC membrane/water interface with the diameter of 1.5 mm and the interfacial area of 0.0177 cm^2. The tube was not used for stripping voltammetry, where a membrane-modified electrode was rotated using a modulated speed rotator (Pine Research Instrumentation). A preconcentration potential was set near the limit of the potential window so that a liming current, i_l, was obtained by rotating-electrode voltammetry. A potential sweep rate during a stripping step was slow enough to exhaustively transfer preconcentrated ions from the PVC membrane into the aqueous sample.

3.3.4 Electrochemical Impedance Spectroscopy (EIS)

EIS was carried out using CHI 660b electrochemical workstation (CH Instruments). In cell 1 or 2 without analyte ions, the center of the membrane surface was vertically directed toward the center of a 2 mm diameter Pt counter electrode. The distance between the working and counter electrodes was set to 9 mm. A constant dc bias was applied to the membrane-modified electrode such that no ion transfer occurs across the PVC membrane/water interface. The ac component of the potential was 20 mV (peak-to-peak), and the ac frequency was swept in the range from 10 Hz to 100 kHz.

3.4 RESULTS AND DISCUSSION

3.4.1 Voltammetric Cation Detection with a PVC/PEDOT-Modified

An oxidatively doped PEDOT film was newly introduced to enable voltammetric cation detection with a thin PVC membrane supported on a conducting-polymer-modified electrode (Figure 1b) while voltammetry of anionic analytes, heparin[19] and perchlorate,[18,19] has been reported by employing an undoped POT film (Figure 1a). A PVC/PEDOT-modified Au electrode was employed to detect tetraalkylammoniums with different alkyl groups, i.e., TPA and TEA, as model cationic analytes with different lipophilicities. Well-defined cyclic voltammograms (CVs) of TPA and TEA were obtained at a PVC/PEDOTmodified electrode (red lines in parts a and b of Figure 2, respectively). More lipophilic TPA is transferred more favorably from the aqueous phase into the membrane phase, thereby yielding the corresponding CV at less negative potentials. A peakshaped forward wave based on simple ion transfer from the aqueous phase into the membrane phase is coupled with reduction of the underlying PEDOT film in the oxidized form (Figure 1b). Cation transfer during the reverse potential sweep also gives a peak current response, which requires oxidation of the reduced PEDOT film. Noticeably, the shapes of the CVs indicate that the currents are limited by diffusion-controlled ion transfer at the PVC membrane/water interface rather than by electrolysis of the surface-confined PEDOT film, indicating that this conducting polymer has sufficient redox capacity.[19]

Intrinsic lipophilicities of the tetraalkylammoniums were quantitatively assessed as formal ion-transfer potentials, $\Delta_W^{PVC}\phi_i^{0'}$, from the corresponding CVs. The experimental CVs at a PVC/PEDOT-modified electrode were fitted with CVs simulated for reversible transfer of a monocation (black circles in Figure 2) by the finite element method as reported elsewhere18 (see

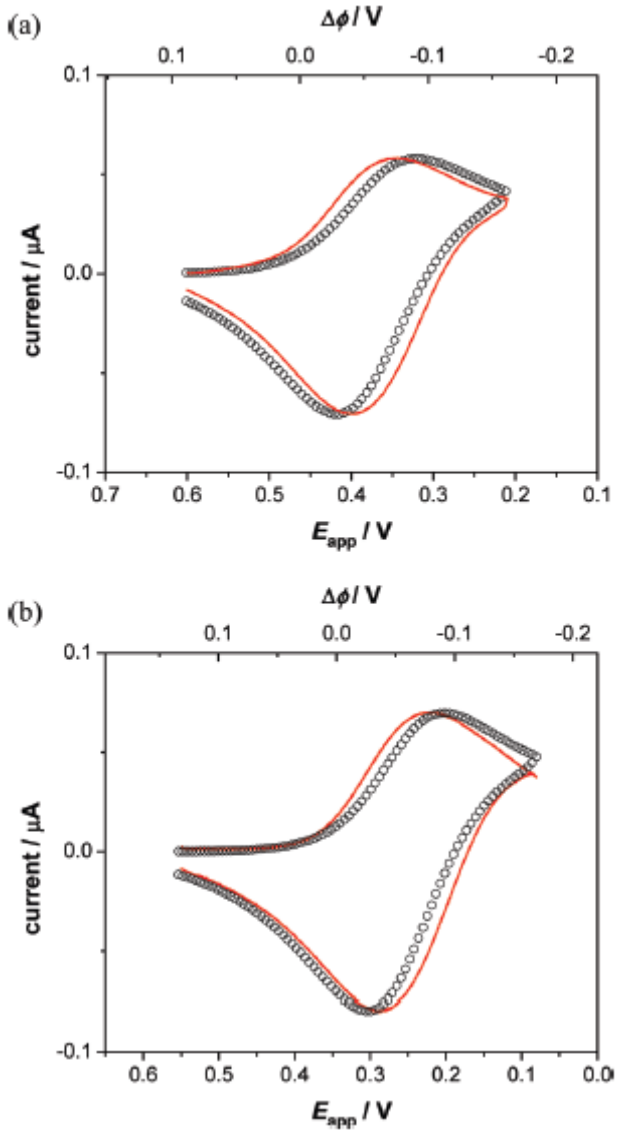

Figure 3-2. Experimental (red line) and simulated (circles) CVs of 20 μM (a) TPA and (b) TEA with a PVC/PEDOT-modified electrode. Scan rate, 0.1 V/s. E_{app} on the bottom axis was converted to $\Delta\phi$ on the top axis by assuming $\partial\Delta_W^{PVC}\phi / \partial E_{app}$ = 0.64 (see Supporting Information).

also Supporting Information). The relatively good fits confirm that the current is limited by ion transfer rather than by PEDOT electrolysis. The fits show that the difference in lipophilicities of TPA and TEA corresponds to the difference of 70 mV in their formal ion-transfer potentials. In this analysis, the potential applied to the Au electrode, E_{app}, was converted to the potential applied at the PVC membrane/water interface (indicated as $\Delta\Phi$ on the top axis of Figure 2) by considering polarization of a PVC/PEDOT/Au junction (see Supporting Information).[18,19] The polarization at the PEDOT-based system, however, does not exactly follow an empirical relationship (see eq S2 in the Supporting Information), thereby causing the deviation between the experimental and simulated CVs of TEA and TPA transfers. This deviation is not due to an Ohmic potential drop in the membrane, which is sufficiently conductive as demonstrated later by EIS.

The CVs of TPA and TEA also demonstrate that the solidsupported membrane is thin enough for these tetraalkylammoniums to be exhaustively stripped from the membrane during the reverse potential sweep at 0.1 V/s. In fact, the total charge under the forward response in the CVs (0.15 and 0.12 μC for TPA and TEA, respectively) is nearly canceled by the total charge under the reverse response (0.14 and 0.11 μC for the respective ions). Moreover, the resulting reverse peak current is enhanced by efficient ion diffusion in the thin membrane to be larger than the forward peak current, which contrasts to the corresponding peak currents based on semi-infinite ion diffusion in a thick membrane. The modes of membrane ion diffusion are characterized by a dimensionless parameter, σ, as[18]

Equation 3-7
$$\sigma = \frac{l^2 |z_i| F v}{D_m R T}$$

where v is a potential sweep rate and D_m is a diffusion coefficient of the transferred ions in the membrane phase. The numerical analysis of the experimental CVs of TPA and TEA gives σ

values of 6.3 and 4.7, respectively, which are much smaller than a σ value of >100 for semi-infinite ion diffusion. These σ values of TPA and TEA, however, are larger than required for an idealistic thin layer behavior (σ < 1), where diffusion of an analyte ion in the membrane is negligible.[18] The intermediate σ values of a PVC/PEDOT-modified electrode are due to a relatively thick PVC membrane, which must be at least as thick as 3 μm to completely cover a PEDOT film.

3.4.2 Preconcentration of Tetraalkylammoniums with Different Lipophilicities

More lipophilic TPA with a less negative formal potential gives a larger preconcentration factor, Y (eq 2), thereby resulting in a larger time constant for preconcentration of TPA. In fact, equilibrium preconcentration of TPA takes longer as proved by measuring stripping voltammograms of TPA and TEA at different preconcentration times. Stripping voltammograms of 25 nM TPA demonstrate that peak current responses vary with preconcentration times even after 1 h (Figure 3a). On the other hand, a stripping response to 250 nM TEA reaches a plateau only after ~2 min preconcentration (data not shown) when equilibrium partitioning of TEA between the membrane and aqueous phases is achieved.

The remarkably different time profiles for preconcentration of TPA and TEA are quantitatively ascribed to their different lipophilicities as represented by a preconcentration factor, Y. The integrations of the stripping voltammograms for TPA and TEA give the total charge based on preconcentrated analyte ions, $Q(t_p)$, which is plotted against preconcentration time, t_p (Figure 3b). The plots for TPA and TEA fit well with eq 3, thereby yielding equilibrium charges, Q_{eq}, as well as time constants, Q_{eq}/i_l. The good fits confirm that the nonequilibrium preconcentration processes limited by mass transfer of an ion in the aqueous solution is well

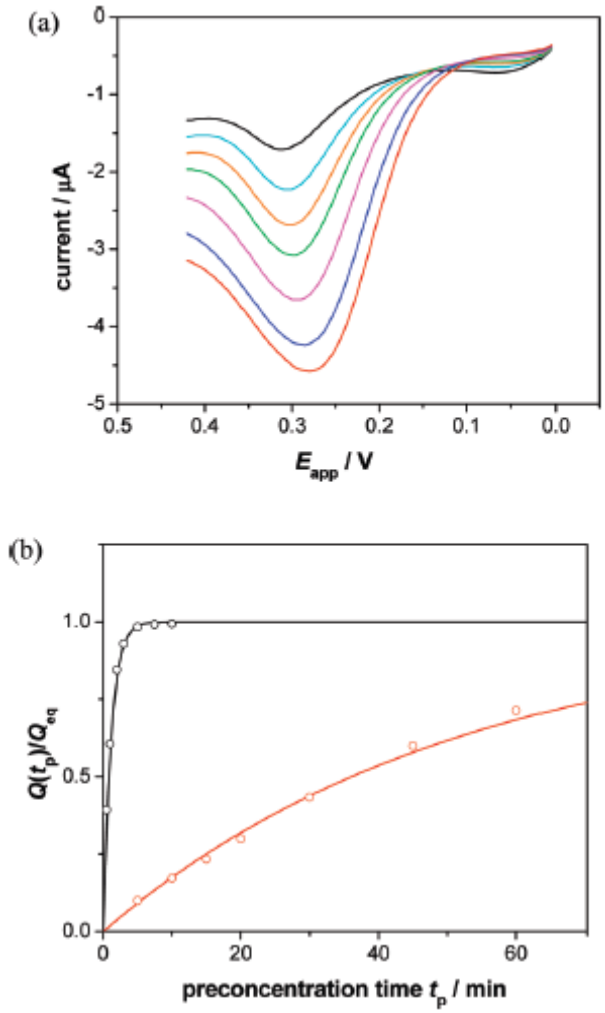

Figure 3-3. (a) Stripping voltammograms of 25 nM TPA at 0.1 V/s after preconcentration for 5 (black), 10 (cyan), 15 (orange), 20 (green), 30 (magenta), 45 (blue), and 60 (red) min. A PVC/PEDOT-modified electrode was rotated at 4000 rpm. (b) Plots of $Q(t_p)/Q_{eq}$ versus t_p for TPA (red) and TEA (black). The circles and solid lines represent experimental and theoretical (eq 3) values, respectively

controlled under the rotating electrode configuration.[18] Q_{eq} values for the respective ions correspond to applied potentials of $\Delta_W^{PVC}\phi - \Delta_W^{PVC}\phi_i^{0'}$ = 0.31 ± 0.01 and 0.23 ± 0.01 V as obtained by using eqs 2 and 4 with l) 3 μm. Since the same potential was applied for preconcentration of both TPA and TEA, the different applied potentials correspond to the difference of 0.08 ± 0.01 V in formal potentials of the two ions. This result agrees well with the difference of the formal potentials determined by cyclic voltammetry (see above). Equation 2 with these applied potentials gives Y = (1.6 ± 0.7) × 10^5 and (1.0 ± 0.4) × 10^4 for TPA and TEA, respectively, indicating that the PVC membrane has 16 times higher capacity for more lipophilic TPA at the preconcentration potential. It should be noted that the remarkably different time profiles for preconcentration of 25 nM TPA and 250 nM TEA in Figure 3b are not due to the different aqueous concentrations, which do not affect a preconcentration time constant, Q_{eq}/i_l, in eq 6 (2.3 × 10^3 and 7.5 × 10 s for TPA and TEA, respectively). In fact, a higher concentration was needed for TEA because of lower sensitivity to this less lipophilic analyte (see below).

3.4.3 Subnanomolar LOD for Tetrapropylammonium by Stripping Voltammetry

Stripping voltammetry with a PVC/PEDOT-modified electrode gives a subnanomolar LOD for TPA after 30 min preconcentration. The resulting current responses to TPA vary with its concentrations in the range of 50-1000 pM (Figure 4a). The IUPAC's upper limit approach[31] was employed to obtain a LOD of (8 ± 4) × 10^{-11} M TPA at a confidence level of 95% from a linear relationship between the stripping peak current and TPA concentration (Figure 4b). This LOD is the lowest value reported so far for ion-transfer stripping voltammetry. The LOD for TPA is not significantly lowered by increasing the preconcentration time from 30 min, at which the concentration of TPA in the membrane reaches 43% of the equilibrium concentration (Figure 3b).

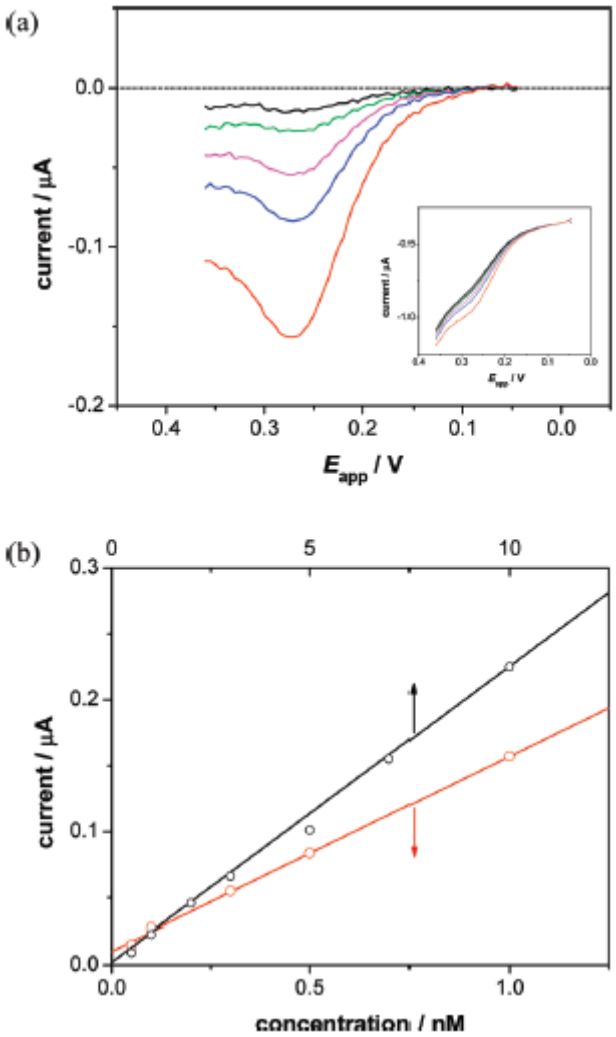

Figure 3-4. Background-subtracted stripping voltammograms of 50 (black), 100 (green), 300 (magenta), 500 (blue), and 1000 (red) pM TPA in deionized water at 0.1 V/s after 30 min preconcentration. The inset shows original stripping voltammograms including a background stripping voltammogram. A PVC/PEDOT-modified electrode was rotated at 4000 rpm. (b) Plots of background-subtracted peak current versus TPA concentrations after 3 (black circles) and 30 min (red circles) preconcentration. The solid lines represent the best fits used for determination of LODs.

A much higher LOD of 0.44 nM TPA was obtained by reducing the preconcentration time to 3 min (Figure 4b). On the other hand, a stripping peak current varies linearly with TEA concentrations only at >0.5 nM after either 3 or 30 min preconcentration, thereby yielding LODs of 0.37 and 0.42 nM, respectively. A PVC membrane is saturated with TEA after ~2 min preconcentration (Figure 3b) so that longer preconcentration does not increase the membrane concentration of TEA or, subsequently, lower the LOD. Overall, the lower LOD for TPA in comparison to the LODs for TEA is consistent with higher lipophilicity of TPA as expected from its larger *Y* value (Table 1). The LOD for TPA, however, is only ~5 times lower while the preconcentration factor, *Y*, for TPA is 16 times larger. The apparently moderate LOD for TPA is due to increasing background current in this potential range (inset of Figure 4a).

It should be noted that a lower LOD for TPA at a long preconcentration time of 30 min is also advantageous for its detection in the presence of TEA. A stripping voltammogram with a mixed solution of TEA and TPA at the identical concentration is dominated by a response to TPA around ~0.3 V after 30 min preconcentration (left voltammogram in Figure 5). This apparently high selectivity for TPA over TEA is due to immediate saturation of a PVC membrane with less lipophilic TEA at the early stage of a preconcentration step while TPA is steadily preconcentrated into the membrane for 30 min to give a much larger stripping current response. On the other hand, a significant stripping response to TEA is observed around ~0.19 V after 30 s preconcentration (right voltammogram in Figure 5), which is resolved from the response to TPA, because of their different formal potentials.

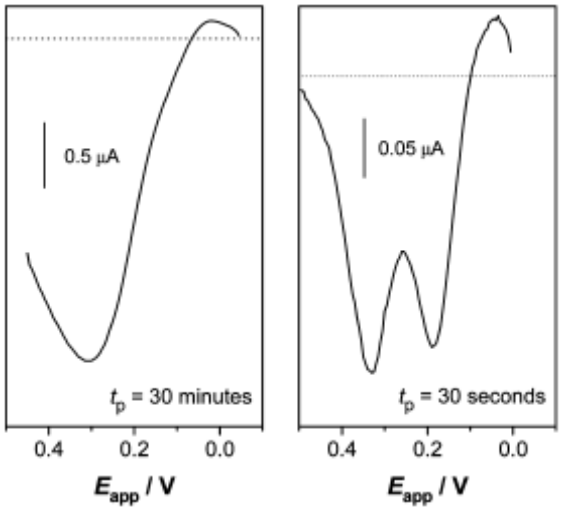

Figure 3-5. Background-subtracted stripping voltammograms of TEA and TPA in a mixed solution at the identical concentration after preconcentration for 30 min (left) and 30 s (right). The ion concentrations are 25 and 50 nM, respectively. The dotted lines represent zero current.

3.4.4 Hexafluoroarsenate as a Lipophilic Anionic Contaminant

Hexafluoroarsenate was investigated as one of the most lipophilic inorganic anions in the so-called Hofmeister series[32] to demonstrate that a subnanomolar LOD is obtained also for a lipophilic anion. Hexafluoroarsenate is an arsenical biocide[25] used as a pesticide, Hexaflurate.[24] Hexafluoroarsenate was recently found in wastewater from a crystal glass factory containing high concentrations of arsenic and fluoride.[26,27]

A well-defined CV of lipophilic hexafluoroarsenate was obtained favorably with a PVC/POT-modified electrode (Figure 6). The CV fits very well with a CV simulated for reversible anion transfer, which controls measured currents. A σ value of <1 as obtained from the fit indicates that the solid-supported membrane serves as a thin-layer cell.[18] This σ value for hexafluoroarsenate with a PVC/POT-modified electrode is smaller than σ values obtained for TEA and TPA with a PVC/PEDOT modified electrode, because a PVC membrane of the former electrode is thinner than that of the latter (l = 0.718 and 3 μm in eq 7, respectively). The numerical analysis also gives a formal potential of hexafluoroarsenate, which is by 61 mV less positive than that of less lipophilic perchlorate.[18]

The higher lipophilicity of hexafluoroarsenate is confirmed by stripping voltammetry of 25 nM hexafluoroarsenate at various preconcentration times (Figure 7a). The stripping current response increases monotonically at a longer preconcentration time to reach a plateau value within 20 min preconcentration when equilibrium partitioning of hexafluoroarsenate between the membrane and aqueous phases is achieved. The preconcentration time required for equilibration is ~10 times longer than that for perchlorate,[18] which is due to higher lipophilicity of hexafluoroarsenate (eq 6). A plot of $Q(t_p)/Q_{eq}$ versus t_p for hexafluoroarsenate fits well with eq 3

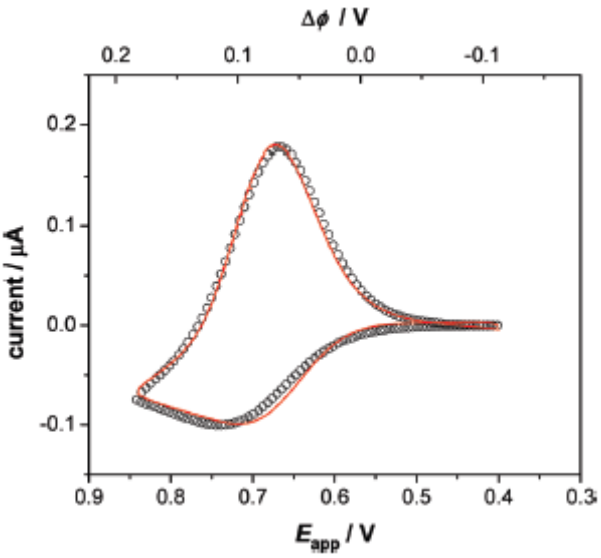

Figure 3-6. Experimental (red line) and simulated (circles) CVs of 20.4 μM hexafluoroarsenate at a PVC/POT-modified electrode. Scan rate, 0.1 V/s. E_{app} on the bottom axis was converted to $\Delta\phi$ on the top axis by assuming $\partial\Delta_W^{PVC}\phi / \partial E_{app}$ = 0.67 (see Supporting Information).

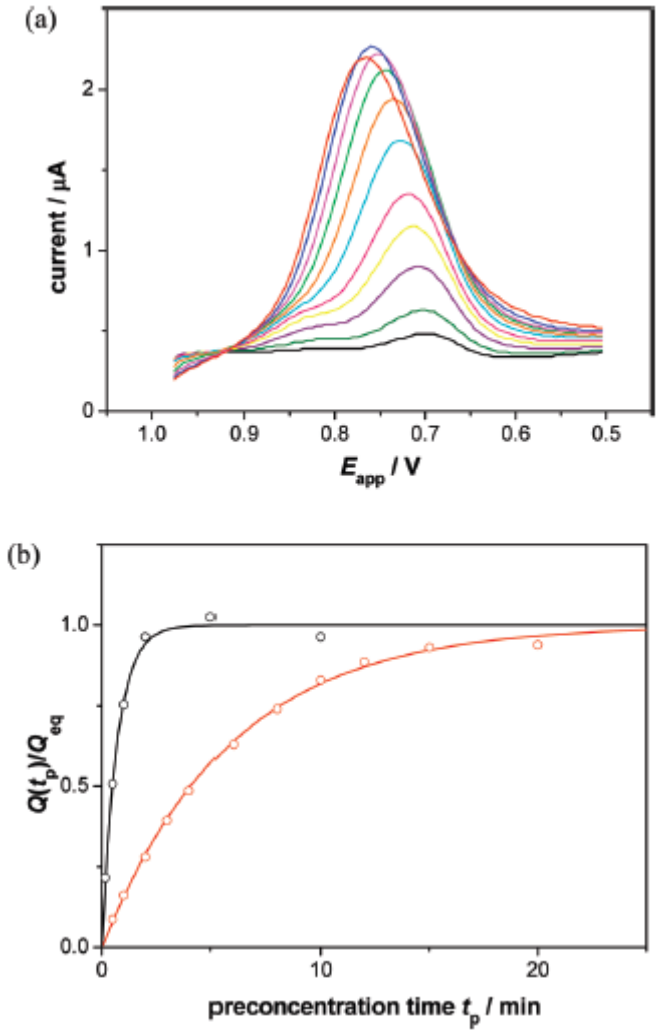

Figure 3-7. (a) Stripping voltammograms of 25 nM hexafluoroarsenate at 0.1 V/s after a preconcentration step of 0.5 (black), 1 (olive), 2 (purple), 3 (yellow), 4 (pink), 6 (cyan), 8 (orange), 10 (green), 12 (magenta), 15 (blue), and 20 (red) min. A PVC/POT electrode was rotated at 4000 rpm. (b) Plots of $Q(t_p)/Q_{eq}$ versus t_p for hexafluoroarsenate (red) and perchlorate (black). The circles and solid lines represent experimental and theoretical (eq 3) values, respectively.

(Figure 7b) to give a Q_{eq} value, which corresponds to an applied potential of 0.31 V with respect to a formal potential as given by using eqs 2 and 4 with l =0.7 μm. This applied potential is more positive than the corresponding applied potential of 0.25 V for perchlorate by 60 mV, which is consistent with the difference in formal potentials of hexafluoroarsenate and perchlorate as determined by cyclic voltammetry. Consequently, the corresponding Y value of hexafluoroarsenate is 12 times larger than that of perchlorate (Table 1). It should be noted that, despite similar applied potentials and, subsequently, preconcentration factors for TPA and hexafluoroarsenate, a thinner PVC membrane covered on a POT-modified electrode is more quickly saturated with hexafluoroarsenate than a PVC/PEDOT membrane with TPA (Figures 3b and 7b, respectively) as expected from the dependence of the preconcentration time constant on the membrane thickness (eq 6).

3.4.5 Subnanomolar LOD for Hexafluoroarsenate by Stripping Voltammetry

A subnanomolar LOD for hexafluoroarsenate was obtained by stripping voltammetry with a PVC/POT-modified electrode in deionized water containing 0.01 M Li_2SO_4. Stripping current responses after 8 min preconcentration vary with 0.25-1.25 nM hexafluoroarsenate (Figure 8). The backgroundsubtracted peak current is linear to the sample ion concentration (inset of Figure 8). A LOD of $(9 \pm 2) \times 10^{-11}$ M was obtained by using the IUPAC's upper limit approach at a confidence level of 95%.31 This LOD is comparable to the LOD of 80 pM hexafluoroarsenate (6 ng/L as arsenic) in waters by inductively coupled plasma mass spectrometry with anion-exchange chromatography.[33] Moreover, the LOD for hexafluoroarsenate with a PVC/POT-modified electrode in 0.01 M Li_2SO_4 is significantly lower than the corresponding LOD of 0.5 ± 0.1 nM perchlorate, to which stripping current responses vary with its concentrations only at ≥1

nM.[18] The lower LOD for more lipophilic hexafluoroarsenate is expected from its larger *Y* value (Table 1). In fact, the higher lipophilicity of hexafluoroarsenate is shown also in the stripping voltammograms (Figure 8), where the background peak current responses around ~0.87 V are due to perchlorate contaminated in the membrane during electrochemical deposition of a POT film in 0.5 M $LiClO_4$.[18] Overall, LODs of both cations and anions examined in this study are mainly dictated by their lipophilicities as quantified by their *Y* values (see Table 1).

3.4.6 EIS of Membrane-Modified Electrodes

Ac impedance responses of PVC/PEDOT- and PVC/POT-modified electrodes confirm that these thin double-polymer membranes are conductive enough to avoid a significant Ohmic potential drop in the membranes. A membrane-modified electrode was immersed in 0.01 M Li_2SO_4 and biased with a dc potential such that no ion transfer occurs across the PVC membrane/water interface. For the blocking electrode, the impedance, *Z*, can be expressed by use of a resistor and a constant phase element as[34]

Equation 3-8
$$Z = Z_{\mathrm{Re}} - jZ_{\mathrm{Im}} = R + \frac{1}{(j\omega)^{\alpha} Q}$$

where *R*, α, and *Q* are real values and independent of the ac frequency, ω, of potential. Equation 8 fits well with impedance responses in low frequency regions ($R < Z_{\mathrm{Re}}$ in Figure 8), thereby yielding the corresponding parameters listed in Table 2. The following discussion is focused on the resistance, *R*, which represents the sum of resistances in the bulk membrane and aqueous phases. Interpretation of the constant phase element can be hardly made because of the presence of multiple interfaces in the membrane-modified electrodes.

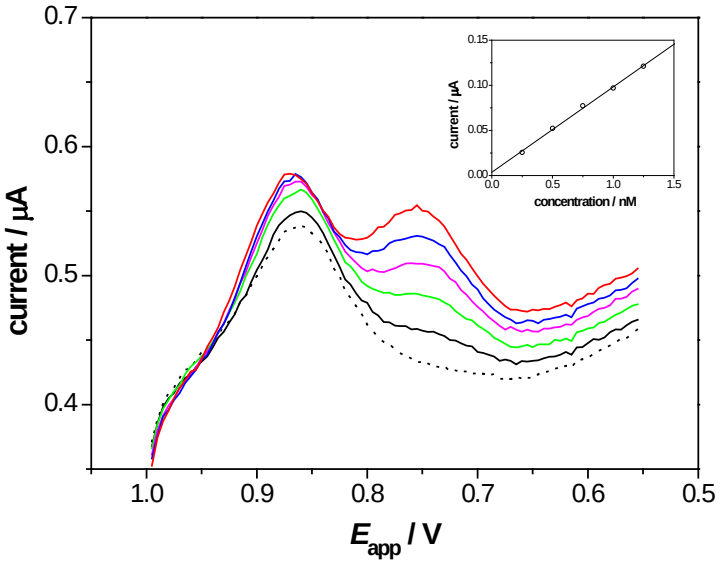

Figure 3-8. Stripping voltammograms of 0 (black dotted), 0.25 (black solid), 0.5 (green), 0.75 (magenta), 1 (blue), and 1.25 (red) nM hexafluoroarsenate at 0.1 V/s. The inset shows a plot of background-subtracted peak current versus analyte concentration. The solid line represents the best fit used for determination of LODs. Preconcentration time was 8 min. A PVC/POT-modified electrode was rotated at 4000 rpm.

The *R* values with the membrane-modified electrodes are similar to the *R* value with a bare Au electrode (Table 2), indicating that the *R* values mainly reflect the solution resistance between the working and counter electrodes. The *R* value with the PVC/PEDOT-modified electrode is larger than that with the bare Au electrode only by 0.06 kΩ, which corresponds to the resistance of the PVC/PEDOT membrane. Despite a thinner PVC membrane, the *R* value with the PVC/POT-modified electrode is larger than that with the PVC-PEDOT-modified electrode by 0.08 kΩ. This result indicates that the undoped POT film is more resistive than the oxidatively doped PEDOT film. Both membrane resistances of <0.15 kΩ and total resistances of ≤0.60 kΩ are small enough to cause a negligible Ohmic potential drop of < 1 mV in the membranes when stripping current of <1.5 μA flows across the membranes under the experimental conditions employed in this study.

It should also be noted that impedance responses of membrane-modified and bare Au electrodes in lower frequency regions ($R << Z_{\mathrm{Re}}$) depend on the dc component of potential such that α values are affected (data not shown). Impedance responses in higher frequency regions ($Z_{\mathrm{Re}} \approx R$ or lower) are rather independent of the dc bias, thereby yielding similar *R* values as listed in Table 2. We were not able to find a good equivalent circuit for the impedance responses in the higher frequency regions, where data points are limited by the available frequency range of our instrument (Figure 8b).

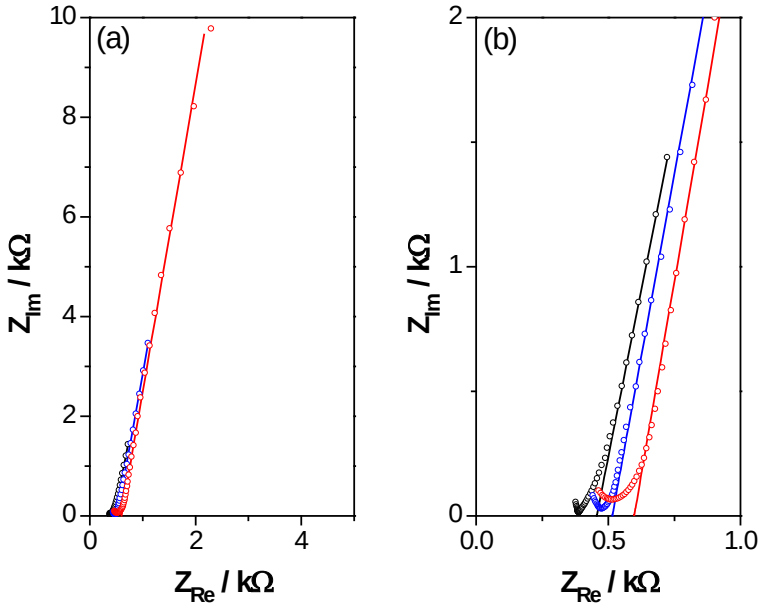

Figure 3-9. Nyquist plots of experimental (circles) and simulated (solid lines) impedance responses in the (a) whole and (b) higher frequency regions as obtained with PVC/POT-modified (red), PVC/PEDOT-modified (blue), and bare (black) Au electrodes in 0.01 M Li_2SO_4. The dc biases applied to the respective electrodes were 0.15, 0, and 0 V against a Ag/AgCl reference electrode. An equivalent circuit based on a constant phase element was used for the simulations.

Table 2. Parameters Determined from Impedance Responses of Membrane-Modified and Bare Au Electrodes in 0.01 M Li_2SO_4.

electrode	R / kΩ	α	Q^a
PVC/PEDOT[b]	0.52	0.89	1.6×10^5
PVC/POT[b]	0.60	0.90	4.8×10^5
bare	0.46	0.88	6.7×10^4

[a] The unit depends on α.[34] [b] A PVC membrane was spin-coated on a conducting polymer-modified Au electrode with 5 mm diameter as described in the Experimental section.

3.5 CONCLUSION

The subnanomolar LODs that were obtained for both cationic and anionic analytes by employing PVC/PEDOT- and PVC/POT-modified electrodes, respectively, are the lowest LODs reported so far for ion-transfer stripping voltammetry. The subnanomolar LODs were obtained for lipophilic ions as predicted by eq 2. The great sensitivity for lipophilic ions is potentially useful for environmental analysis because high lipophilicity of an ion is relevant to its bioaccumulation and toxicity. Hexafluoroarsenate[32] and perchlorate[35] are two of the most lipophilic inorganic anions in the Hofmeister series. Moreover, we have recently employed ion-transfer voltammetry to demonstrate that perfluoroalkyl carboxylate and sulfonate, which are an emerging class of organic contaminants,[36] are much more lipophilic than their alkyl counterparts.[37] Other lipophilic ions that potentially possess adverse health effects include ionizable pharmaceuticals[38] and ionic liquids.[39] These ions are detectable also by ion-transfer voltammetry.[40-42]

The subnanomolar LODs represent practical limits for monovalent ions. An even lower LOD as expected for a more lipophilic monovalent ion requires extremely long preconcentration (>>1 hr). On the other hand, an ion with a larger charge will give a lower LOD without prolonged preconcentration, because stripping currents based on a thin-layer behavior vary with the square of the charge number.[43] Picomolar LODs are expected for ion-transfer stripping voltammetry based on facilitated extraction of polyions, e.g., polypeptide protamine (~+20)[44-46] and pentasaccharide Arixtra (~–10).[47] The extremely high sensitivity may be useful for detection of these biological polyions in complicated biological and biomedical samples such as whole blood, where a liquid/liquid interface is fouled to lower voltammetric sensitivity.[16]

Voltammetric cation detection with a thin polymeric membrane supported on a conducting-polymer-modified electrode was demonstrated for the first time by employing a PEDOT film. In contrast to anionic analytes, many ionophores with excellent selectivity among cations were developed for potentiometry.[48] These highly selective ionophores will significantly widen the range of applications of PVC/PEDOT-modified electrodes. On the other hand, a LOD for either cation or anion as obtained with a PVC/PEDOT- or PVC/POT-modified electrode, respectively, is ultimately dictated by the Nernst equation (eq 2). In this regard, our voltammetric approach contrasts to a recent potentiometric approach with a PVC/PEDOT-modified electrode.[49] In the latter approach, both cationic analytes and their co-ions are galvanostatically extracted into a PVC membrane to inevitably obtain a non-equilibrium super-Nernstian response. A LOD of such a non-selective potentiometric response is compromised in comparison to a LOD of an equilibrium, selective Nernstian response.[50]

ACKNOWLEDGEMENTS

This work was supported by a CAREER award from the National Science Foundation (CHE-0645623).

SUPPORTING INFORMATION

Finite Element Simulation of CVs

CVs at PVC/POT- and PVC/PEDOT-modified electrodes were numerically analyzed by employing the finite element method as reported elsewhere.[S1] Specifically, CVs were simulated by using COMSOL Multiphysics version 3.5a (COMSOL, Inc., Burlington, MA. An example of the finite element simulation is attached.

A current response was simulated as a function of the potential drop at the PVC membrane/water interface, $\Delta_{\mathrm{w}}^{\mathrm{PVC}}\phi$. An experimental CV, however, is obtained against the potential applied to the underlying gold electrode, E_{app}, which is also used for a redox reaction of a conducting-polymer film as given by

$$E_{\mathrm{app}} = \Delta_{\mathrm{PVC}}^{\mathrm{Au}}\phi + \Delta_{\mathrm{w}}^{\mathrm{PVC}}\phi - E_{\mathrm{ref}} \qquad \text{(S1)}$$

where $\Delta_{\mathrm{PVC}}^{\mathrm{Au}}\phi$ is the potential drop across the PVC/conducting polymer/gold junction, and E_{ref} is the reference electrode potential. In our previous work,[S1,S2] a linear relationship between $\Delta_{\mathrm{w}}^{\mathrm{PVC}}\phi$ and E_{app} was observed empirically for PVC/POT-modified gold electrodes. With this empirical relationship of a constant value of $\partial\Delta_{\mathrm{w}}^{\mathrm{PVC}}\phi / \partial E_{\mathrm{app}}$, eq S1 is equivalent to

$$\Delta\phi = \Delta_{\mathrm{w}}^{\mathrm{PVC}}\phi - \Delta_{\mathrm{w}}^{\mathrm{PVC}}\phi_{\mathrm{i}}^{0'} = (E_{\mathrm{app}} - E_{\mathrm{i}}^{0'})\frac{\partial\Delta_{\mathrm{w}}^{\mathrm{PVC}}\phi}{\partial E_{\mathrm{app}}} \quad \text{(S2)}$$

where $E_{\mathrm{i}}^{0'}$ is the applied potential at $\Delta_{\mathrm{w}}^{\mathrm{PVC}}\phi = \Delta_{\mathrm{w}}^{\mathrm{PVC}}\phi_{\mathrm{i}}^{0'}$. In the analysis of CVs in Figures 2 and 5, $\partial\Delta_{\mathrm{w}}^{\mathrm{PVC}}\phi / \partial E_{\mathrm{app}}$ was assumed to be same for two ions i and j so that the difference of their formal potentials is given by

$$\Delta_{\mathrm{w}}^{\mathrm{PVC}}\phi_{\mathrm{j}}^{0'} - \Delta_{\mathrm{w}}^{\mathrm{PVC}}\phi_{\mathrm{i}}^{0'} = (E_{\mathrm{j}}^{0'} - E_{\mathrm{i}}^{0'})\frac{\partial\Delta_{\mathrm{w}}^{\mathrm{PVC}}\phi}{\partial E_{\mathrm{app}}} \quad \text{(S3)}$$

It should also be noted that this assumption may be an origin of the deviation between experimental and simulated CVs for a PVC/PEDOT-modified electrode in Figure 2. In contrast, a good fit is obtained for a PVC/POT-modified electrode by using this assumption (Figure 5).[S1,S2]

Supporting Information References

(S1) Kim, Y.; Amemiya, S. *Anal. Chem.* **2008**, *80*, 6056–6065.

(S2) Guo, J.; Amemiya, S. *Anal. Chem.* **2006**, *78*, 6893–6902.

COMSOL Model

A copy of the COMSOL model is available free of charge in the Supporting Information via the Internet at http://pubs.acs.org/doi/suppl/10.1021/ac900995a.

REFERENCES

(1) Samec, Z.; Samcová, E.; Girault, H. H. *Talanta* **2004**, *63*, 21–32.

(2) Wang, J. *Stripping Analysis: Principles, Instrumentation, and Applications*; VCH: Deerfield Beach, FL, 1985.

(3) Wang, J. In *Laboratory Techniques in Electroanalytical Chemistry*, 2nd ed.; Kissinger, P. T., Heineman, W. R., Eds.; Marcel Dekker: New York, 1996, pp 719–737.

(4) Senda, M.; Katano, H.; Kubota, Y. *Collect. Czech. Chem. Commun.* **2001**, *66*, 445–455.

(5) Marecek, V.; Samec, Z. *Anal. Lett.* **1981**, *14*, 1241–1253.

(6) Marecek, V.; Samec, Z. *Anal. Chim. Acta* **1982**, *141*, 65–72.

(7) Marecek, V.; Samec, Z. *Anal. Chim. Acta* **1983**, *151*, 265–269.

(8) Homolka, D.; Marecek, V.; Samec, Z.; Base, K.; Wendt, H. *J. Electroanal. Chem.* **1984**, *163*, 159–170.

(9) Katano, H.; Senda, M. *Anal. Sci.* **1998**, *14*, 63–65.

(10) Katano, H.; Senda, M. *Anal. Sci.* **2001**, *17*, i337–i340.

(11) Senda, M.; Katano, H.; Yamada, M. *J. Electroanal. Chem.* **1999**, *468*, 34–41.

(12) Katano, H.; Senda, M. *J. Electroanal. Chem.* **2001**, *496*, 103–109.

(13) Sherburn, A.; Arrigan, D. W. M.; Dryfe, R. A. W.; Boag, N. M. *Electroanalysis* **2004**, *16*, 1227–1231.

(14) Ohkouchi, T.; Kakutani, T.; Osakai, T.; Senda, M. *Anal. Sci.* **1991**, *7*, 371–376.

(15) Lee, H. J.; Beriet, C.; Girault, H. H. *Anal. Sci.* **1998**, *14*, 71–77.

(16) Guo, J.; Yuan, Y.; Amemiya, S. *Anal. Chem.* **2005**, *77*, 5711–5719.

(17) Collins, C. J.; Arrigan, D. W. M. *Anal. Chem.* **2009**, *81*, 2344–2349.

(18) Kim, Y.; Amemiya, S. *Anal. Chem.* **2008**, *80*, 6056–6065.

(19) Guo, J.; Amemiya, S. *Anal. Chem.* **2006**, *78*, 6893–6902.

(20) *Interim Drinking Water Health Advisory for Perchlorate*; EPA 822-R-08-025; Health and Ecological Criteria Division, Office of Science and Technology, Office of Water, U.S. Environmental Protection Agency: Washington, DC, 2008.

(21) Groenendaal, B. L.; Jonas, F.; Freitag, D.; Pielartzik, H.; Reynolds, J. R. *Adv. Mater. (Weinheim, Ger.)* **2000**, *12*, 481–494.

(22) Groenendaal, L.; Zotti, G.; Aubert, P. H.; Waybright, S. M.; Reynolds, J. R. *Adv. Mater. (Weinheim Ger.)* **2003**, *15*, 855–879.

(23) Hamilton, D. J.; Ambrus, A.; Dieterle, R. M.; Felsot, A. S.; Harris, C. A.; Holland, P. T.; Katayama, A.; Kurihara, N.; Linders, J.; Unsworth, J.; Wong, S. S. *Pure Appl. Chem.* **2003**, *75*, 1123–1155.

(24) Reisinger, H. J.; Burris, D. R.; Hering, J. G. *Environ. Sci. Technol.* **2005**, *39*, 458A–464A.

(25) Daus, B.; von Tumpling, W.; Wennrich, R.; Weiss, H. *Chemosphere* **2007**, *68*, 253–258.

(26) Daus, B.; Weiss, H.; Bernhard, K.; Hoffmann, P.; Neu, T. R.; von Tumpling, W.; Wennrich, R. *Eng. Life Sci.* **2008**, *8*, 598–602.

(27) Bobacka, J.; Ivaska, A.; Lewenstam, A. *Chem. Rev.* **2008**, *108*, 329–351.

(28) Samec, Z. *Pure Appl. Chem.* **2004**, *76*, 2147–2180.

(29) Homolka, D.; Hung, L. Q.; Hofmanova, A.; Khalil, M. W.; Koryta, J.; Marecek, V.; Samec, Z.; Sen, S. K.; Vanysek, P. *Anal. Chem.* **1980**, *52*, 1606–1610.

(30) Bard, A. J.; Faulkner, L. R. *Electrochemical Methods: Fundamentals and Applications*, 2nd ed.; John Wiley and Sons: New York, 2001; p 339.

(31) Mocak, J.; Bond, A. M.; Mitchell, S.; Scollary, G. *Pure Appl. Chem.* **1997**, *69*, 297–328.

(32) Zhang, G.-X.; Imato, T.; Ishibashi, N. *Bunseki Kagaku* **1989**, *38*, 283–285.

(33) Wallschlager, D.; London, J. *J. Anal. At. Spectrom.* **2005**, *20*, 993–995.

(34) Orazem, M. E.; Tribollet, B. *ELectrochemical Impedance Spectroscopy*; John Wiley & Sons: Hobeken, NJ, 2008, pp 233.

(35) Wegmann, D.; Weiss, H.; Ammann, D.; Morf, W. E.; Pretsch, E.; Sugahara, K.; Simon, W. *Mikrochim. Acta* **1984**, *3*, 1–16.

(36) Larsen, B. S.; Kaiser, M. A. *Anal. Chem.* **2007**, *79*, 3966–3973.

(37) Jing, P.; Rodgers, P. R.; Amemiya, S. *J. Am. Chem. Soc.* **2009**, *131*, 2290–2296.

(38) Ternes, T. A. *Trac Trends Anal. Chem.* **2001**, *20*, 419–434.

(39) Jastorff, B.; Stormann, R.; Ranke, J.; Molter, K.; Stock, F.; Oberheitmann, B.; Hoffmann, W.; Hoffmann, J.; Nuchter, M.; Ondruschka, B.; Filser, J. *Green Chem.* **2003**, *5*, 136–142.

(40) Caron, G.; Reymond, F.; Carrupt, P. A.; Girault, H. H.; Testa, B. *Pharm. Sci. Technol. Today* **1999**, *2*, 327–335.

(41) Quinn, B. M.; Ding, Z. F.; Moulton, R.; Bard, A. J. *Langmuir* **2002**, *18*, 1734–1742.

(42) Kakiuchi, T. *Anal. Chem.* **2007**, *79*, 6442–6449.

(43) Bard, A. J.; Faulkner, L. R., 2nd ed.; John Wiley & Sons: New York, 2001, pp 458–464.

(44) Amemiya, S.; Yang, X.; Wazenegger, T. L. *J. Am. Chem. Soc.* **2003**, *125*, 11832–11833.

(45) Yuan, Y.; Amemiya, S. *Anal. Chem.* **2004**, *76*, 6877–6886.

(46) Rodgers, P. J.; Amemiya, S. *Anal. Chem.* **2007**, *79*, 9276–9285.

(47) Rodgers, P. J.; Jing, P.; Kim, Y.; Amemiya, S. *J. Am. Chem. Soc.* **2008**, *130*, 7436–7442.

(48) Umezawa, Y.; Bühlmann, P.; Umezawa, K.; Tohda, K.; Amemiya, S. *Pure Appl. Chem.* **2000**, *72*, 1851–2082

(49) Perera, H.; Fordyce, K.; Shvarev, A. *Anal. Chem.* **2007**, *79*, 4564–4573.

(50) Ceresa, A.; Radu, A.; Peper, S.; Bakker, E.; Pretsch, E. *Anal. Chem.* **2002**, *74*, 4027–4036.

4.0 DOUBLE-POLYMER-MODIFIED PENCIL LEAD FOR STRIPPING VOLTAMMETRY OF PERCHLORATE IN DRINIKING WATER

This work has been published as A. Izadyar, Y. Kim, M. M. Ward, and S. Amemiya, *J. Chem. Educ.*, **2012**, *89*, 1323-1326.

4.1 INTRODUCTION

Recently, significant attention has been given to the environmental and public health effects of perchlorate contamination of drinking water source.[1] The potential health effects associated with perchlorate include the disrupted production of thyroid hormones due to the blocking effect of perchlorate on Na^+/I^- transporter in the thyroid.[2] In the past, perchlorate salts were widely used in the manufacture of munitions, explosives, fireworks, and so forth. Moreover, perchlorate was discovered on Mars by NASA's Phoenix Lander[3] as well as on most continents of earth including Antarctic Dry Valleys,[4] indicating its natural occurrence. In February 2011, the U.S. Environmental Protection Agency (EPA) announced a decision to regulate perchlorate in drinking water, for which an interim health advisory level of 15 ppb (~150 nM) has been set.[5] The present EPA-recommended methods for the trace analysis of perchlorate require highly

sensitive instruments that are commonly unavailable in undergraduate teaching laboratories, such as an electrospray ionization mass spectrometer and a suppressed conductivity detector for liquid or ion chromatography.[1]

Here we introduce a double-polymer-modified pencil lead as an inexpensive and disposable (maintenance free) electrode for upper-division undergraduate instrumental laboratories to enable the simple detection of nanomolar concentrations of perchlorate. The proposed method is based on ion-transfer stripping voltammetry6 through the novel application of pencil lead electrodes, which, in principle, is distinguished from their previous educational applications such as ion-selective potentiometry[7] and anodic-stripping voltammetry.[8] The high perchlorate sensitivity and selectivity of the voltammetric sensor are due to the high lipophilicity of perchlorate in comparison with common inorganic anions in drinking water,[9] which is represented by the Hofmeister series as the measure of the free energy of the hydration of these anions:

$$ClO_4^- > NO_3^- > Br^- > NO_2^- \approx Cl^- > HCO_3^- > H_2PO_4^- \approx F^- \approx SO_4^{2-}$$

Specifically, students fabricate their own electrodes and perform perchlorate analysis in a 3−4 h laboratory session to obtain hands-on experience with the electropolymerization of a conducting polymer film; ion and electron-transfer electrochemistry; and cyclic and stripping voltammetry. In addition, students can use the versatile double-polymer-modified electrodes to detect anions of interest beyond perchlorate and evaluate their lipophilicity as the critical molecular property related to their environmental toxicity[10] and pharmaceutical activity.[11]

4.2 EXPERIMENTAL SECTION

4.2.1 Reagents

3-Octylthiophene, lithium perchlorate, lithium sulfate, tetradodecylammonium bromide (TDDABr), poly(vinyl chloride) (PVC; high molecular weight), 2-nitrophenyl octyl ether (oNPOE), and anhydrous acetonitrile were obtained from Aldrich (Milwaukee, WI). Potassium tetrakis(pentafluorophenyl)borate (KTFAB) was purchased from Boulder Scientific Company (Mead, CO). TDDATFAB was prepared by the metathesis of KTFAB and TDDABr as reported elsewhere.[12]

4.2.2 Fabrication of Pencil Lead Electrode

A pencil lead electrode was fabricated using a super hi-polymer lead (0.7 mm, HB, Pentel of America, Torrance, CA) partially insulated with a FEP (fluorinated ethylene propylene) heat shrink tubing (24 Gauge, heat shrink ratio 1.3:1, Zeus, Orangeburg, SC). As shown in Figure 4 in the Supporting Information, the end of the tubing was sealed using 5-min epoxy (ITW Devcon, Danvers, MA) to minimize the penetration of an acetonitrile solution into the gap between the pencil lead and the tubing during POT (poly(3-octylthiophene)) deposition, thereby maintaining a well-defined electrode area. Additionally, a PTFE-coated Cu wire (polytetrafluoroethylene; 20 WAG, Alpha Wire, Elizabeth, NJ) was attached to the pencil lead electrode using silver epoxy H20E (Epoxy Technology, Inc., Billerica, MA) to facilitate electrode handling. An electrode with a good electrical connection gives a resistance of 1−2 Ω through pencil lead and Cu wire.

Noticeably, no perchlorate response is obtained using the uncoated pencil lead electrode, which proves the necessity of the coating (see below).

4.2.3 Electrochemical Experiments

A computer-controlled CHI 600A electrochemical workstation (CH Instruments, Austin, TX) was used for the electropolymerization of POT by cyclic voltammetry and for ion-transfer stripping voltammetry of perchlorate. The respective voltammetric experiments were performed using the following three electrode cells with a Pt counter electrode

Pt|POT|150 mM 3-octylthiophene and 25 mM TDDATPBA (acetonitrile)|pencil lead (cell 1)

Ag|AgCl|3 M KCl||1 mM Li_2SO_4 (water)||100–1000 nM $LiClO_4$ and 1 mM Li_2SO_4 (water)

|TDDATFAB (oNPOE/PVC membrane)|POT|pencil lead (cell 2)

In cell cell 1, a POT-modified Pt wire served as a stable quasi-reference electrode in acetonitrile,[13] whereas a double junction Ag/AgCl reference electrode was used in cell 2. Typically, a group of three students shared one potentiostat to perform all electrochemical measurements in the laboratory session.

4.2.4 HAZARDS

Acetonitrile is highly flammable, is harmful by ingestion and skin absorption (irritant), affects lungs, blood, kidney, liver, and central nervous system, and causes serious eye damage. Lithium sulfate is also harmful by ingestion and has target body effects on central nervous system, kidney, and cardiovascular system. Lithium perchlorate is an irritant and is not combustible. It, however, is a powerful oxidizing agent and forms explosive mixtures and shock sensitive mixtures with

combustible or easily oxidizable materials. Also, lithium perchlorate decomposes violently or explosively at high temperatures and releases oxygen in fire situation. TDDABr is an irritant. KTFAB is explosive and causes irritation by inhalation and contact with skin and eyes.

4.3 RESULTS AND DISCUSSION

4.3.1 Principle

Figure 1 shows the principle of ion-transfer stripping voltammetry of perchlorate with a PVC/POT-modified pencil lead electrode. The plasticized PVC membrane serves as the reservoir of perchlorate, which is preconcentrated from an aqueous sample, while the POT film is necessary as an ion-toelectron transducer to mediate continuous current flow between the ionically conductive PVC membrane and the electronically conductive solid electrode.9 In the preconcentration step, the POT film is oxidized by the underlying pencil lead electrode upon the application of a sufficiently positive potential to drive the transfer of anionic perchlorate from the aqueous phase into the solid-supported PVC/POT membrane. After sufficiently long preconcentraion (typically 5 min for 100 nM perchlorate), the potential of the pencil lead is linearly swept toward the negative direction, such that the reduction of the oxidized POT film drives the reverse transfer of highly concentrated perchlorate into the aqueous phase, thereby yielding a high stripping current response. Noticeably, the POT membrane is not suitable for the preconcentration of an aqueous cation into the PVC membrane,[12] which requires a conducting polymer that is initially in the stable and readily reducible form, such as an oxidatively doped poly(3,4-ethylenedioxythiophene) membrane.[14]

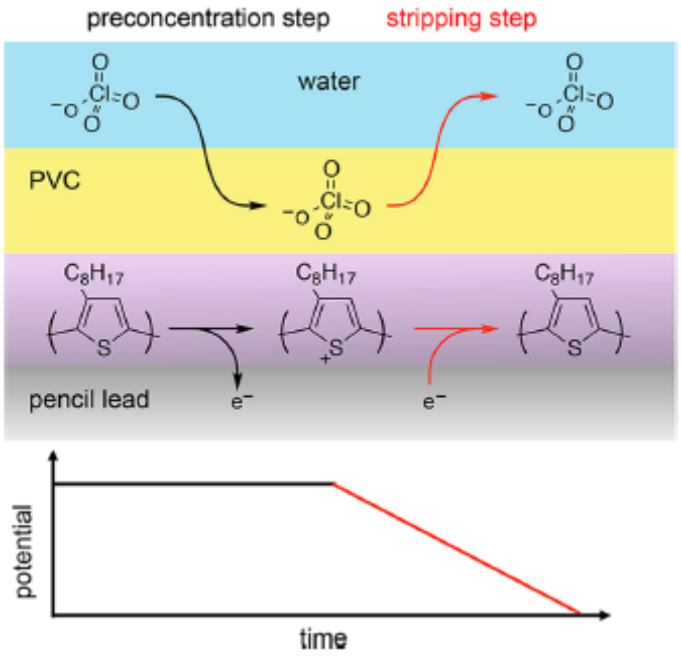

Figure 4-1. Scheme for the preconcentration (black arrows) and stripping (red arrows) of perchlorate at the PVC/POT-modified pencil lead electrode and the corresponding electrode potential (bottom).

4.3.2 Electrode Modification

Students were able to readily prepare their own PVC/POT-modified pencil lead electrodes (Figures 2A and 4 in Supporting Infromation). A pencil lead was partially covered with an FEP heat-shrinkable tubing to expose the graphite surface with a well-defined length of ~5 mm, as shown in Figure 2A. The exposed surface of the pencil lead was coated with a POT membrane through electropolymerization by cyclic voltammetry using cell 1 (Figure 2B). 3-Octylthiophene (OT) was substantially oxidized at >1.25 V, resulting in polymerization at the exposed surface. The growth of the POT membrane with continued cycling of the potential was confirmed by the successive increase in its oxidation and reduction peaks at ~1.0 and ~0.75 V, respectively. Typically, 6 potential cycles produced a POT membrane with adequate redox capacity for stripping voltammetry of nanomolar concentrations of perchlorate (see below). Then, the POTmodified pencil lead electrode was simply dip-coated with a plasticized PVC membrane from a THF solution of PVC, oNPOE as a plasticizer, and TDDATFAB as organic supporting electrolytes (see Supporting Information for the membrane composition) and dried in air (Figure 5 in the Supporting Information).

4.3.3 Stripping Voltammetry of Nanomolar Perchlorate

Stripping voltammetry was performed to analyze standard solutions of 100−1000 nM perchlorate in tap water. Perchlorate, preconcentrated into the PVC membrane for 5 min at 0.83 V, was stripped by linearly sweeping the potential toward the negative direction at 0.1 V/s (Figure 3A). The lack of a significant diffusional tail in the peak-shaped voltammograms indicates that the

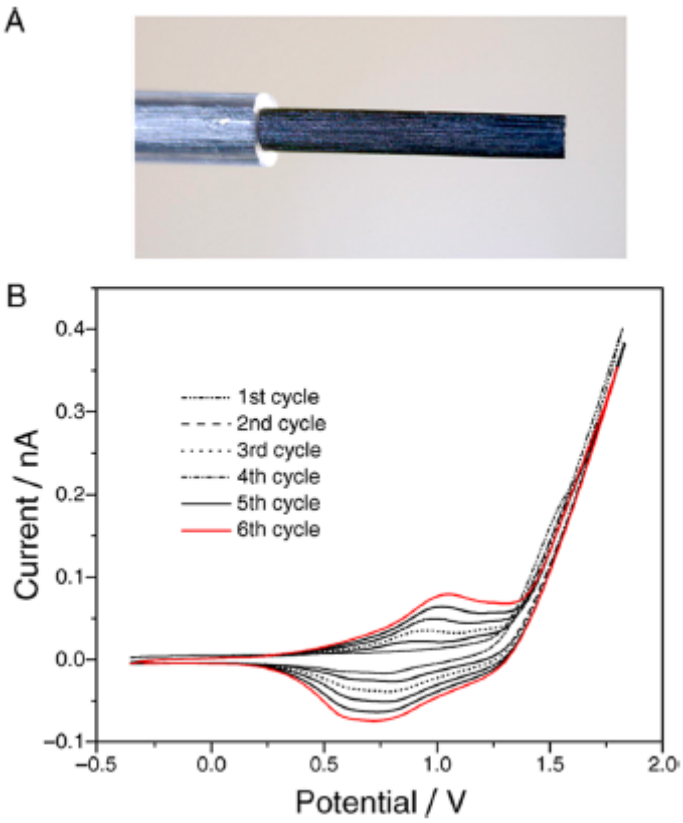

Figure 4-2. (A) Optical image of a PVC/POT-modified pencil lead. (B) CVs of POT deposition on a pencil lead electrode in cell 1. Scan rate, 0.1 V/s.

PVC/POT membrane is thin enough to exhaustively strip the accumulated perchlorate, thereby maximizing the current sensitivity and also keeping the membrane free from perchlorate after each measurement. The stripping peak current is proportional to the aqueous concentration of perchlorate down to 100 nM (Figure 3B), which is lower than the interim health advisory level of 15 ppb (～150 nM) perchlorate in drinking water set by the EPA. This high sensitivity is due to the thermodynamically favorable transfer of perchlorate at the preconcentration potential, which is 0.21 V more positive than the peak potential of 0.63 V for perchlorate stripping. Only perchlorate responses were observed because, as expected from the Hofmeister series, the tap water sample contained no lipophilic interfering anions that would be favorably preconcentrated into the PVC membrane.[9] Moreover, no well-defined peak-shaped response was obtained with the background tap water sample, where a negligible quantity of perchlorate was present. In such a case, the analysis of a spiked unknown sample is recommended (see an example in Supporting Information).

4.3.4 Evaluation of Ion Lipophilicity

If time allows, students are encouraged to study other anions of interest using a PVC/POT-modified pencil lead for their highly sensitive detection as well as for the evaluation of their lipophilicity. In addition to perchlorate, hexafluoroarsenate is also a serious environmental contaminant with sufficiently high lipophilicity[14] to give nanomolar sensitivity (parts B and C of Figure 3). Importantly, the stripping peak potential serves as the quantitative measure of ion lipophilicity; that is, the stripping of a more lipophilic anion is less favorable and therefore requires more negative potentials. The comparison of peak potential for perchlorate (0.63 V in

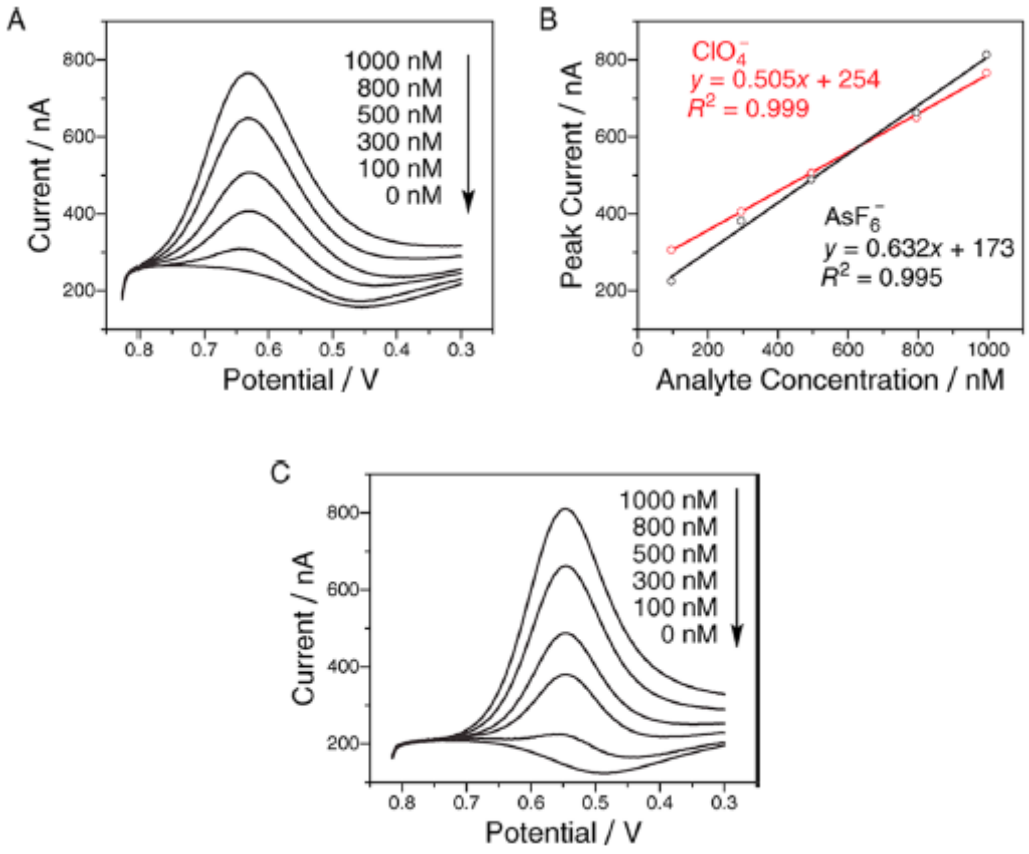

Figure 4-3. Stripping voltammograms of (A) perchlorate and (C) hexafluoroarsenate spiked in tap water and (B) the corresponding plots of peak current versus concentration. Scan rate, 0.1 V/s.

Figures 3A) with that for hexafluoroarsenate (0.55 V in Figure 3C) confirms higher lipophilicity of the latter.

4.4 CONCLUSIONS

The double-polymer-modified pencil lead electrodes are inexpensive, readily fabricated, disposable (maintenance free), and rich in concepts and methodologies of electrochemistry including ion and electron transfers and their coupling, electropolymerization, and cyclic and stripping voltammetry. Students can use their own electrodes to quantitatively address whether their local drinking water is contaminated with nanomolar perchlorate. In addition, students can use a PVC/POT-modified electrode to screen the lipophilicity of various anions, for example, perfluoloalkyl oxoanions[10] and ionized drug molecules,[11] as a physicochemical parameter, which affects their environmental toxicity and pharmaceutical activity, respectively.

ACKNOWLEDGEMENTS

This work was supported by a CAREER award from the National Science Foundation (CHE-0645623). We thank Colin J. Murray, Han Liu, and Joseph G. Plaks for their help in the implementation of double-polymer-modified pencil lead electrodes into the undergraduate instrumental laboratory curriculum.

SUPPORTING INFORMATION

Purpose

The purpose of this experiment is to determine the concentration of perchlorate spiked in tap water by ion-transfer stripping voltammetry using a double-polymer-modified pencil-lead electrode. If time allows, students are encouraged to investigate other anions and evaluate their lipophilicity.

Background

The background information of the proposed perchlorate sensor is detailed in Y. Kim, Y and S. Amemiya, *Anal. Chem.* **2008**, *80*, 6056–6065. Students are encouraged to read this paper and references therein to learn about the environmental contamination of perchlorate, EPA methods for perchlorate analysis, potentiometric and voltammetric ion-selective electrodes for trace analysis, and the theories of the voltammetric ion sensors.

Equipment

A computer-controlled CHI 600A electrochemical workstation (CH Instruments, Austin, TX) was employed for the electropolymerization of poly(3-octyl thiophene) (POT) and for stripping voltammetry of perchlorate. The macro program of the CHI instrument facilitates stripping voltammetric measurements.

Chemicals

3-octylthiophene ($C_{12}H_{20}S$, 65016-62-8)

Lithium perchlorate ($LiClO_4$, 7791-03-9)

Lithium sulfate (Li_2SO_4, 10377-48-7)

Tetradodecylammonium (TDDA) bromide ($C_{48}H_{100}NBr$ 14866-34-3)

Poly(vinyl chloride) (PVC, high molecular weight, 9002-86-2)

2-Nitrophenyl octyl ether (*o*NPOE, $C_{14}H_{21}O_3N$, 37682-29-4)

Acetonitrile (C_2H_3N, 75-05-8)

Potassium tetrakis(pentafluorophenyl)borate (KTFAB, $C_{24}F_{20}BK$, 89171-23-3)

Harzards

The hazard identification of these chemicals is listed in Table 1.

Electrode Materials

Super hi-polymer lead (0.7 mm, HB, Pentel of America, Torrance, CA)

FEP heat shrink tubing (24 Gauge, Heat Shrink Rat 1.3:1, Zeus, Orangeburg, SC)

5 minute epoxy (ITW Devcon, Danvers, MA)

Silver epoxy H20E (Epoxy Technology Inc., Billerica, MA)

PTFE-coated Cu wire (20 WAG, Alpha Wire, Elizabeth, NJ)

Table 4-1. Hazard Identification

chemicals	health hazard	flammability	physical hazards
3-octylthiophene	0	1	0
lithium perchlorate	2	0	0
lithium sulfate	1	0	2
TDDABr	2	0	0
PVC	2	0	0
*o*NPOE	1	1	0
acetonitrile	2	3	0
KTFAB	2	1	3

Pencil-Lead Electrode

1. Cut a pencil lead into two equal parts (3.0 cm each).

2. Cut a 2.0 cm-long FEP heat shrinkable tube.

3. Cut a 5.0 cm-long copper wire.

4. Cover the pencil-lead by tube to expose 4 mm from the uncut end.

5. Attach the copper wire to the cut end of the pencil lead using silver epoxy.

6. Keep the electrode at 100°C in the oven for 30 minutes to cure the epoxy and also shrink the tube.

7. After cooling the electrode, use 5 min epoxy to seal the heat shrinkable tube at the side near the Cu wire. This sealing is needed to avoid the penetration of acetonitrile into the gap between the pencil lead and the FEP tube, which causes an ill-defined electrode area.

8. Keep the electrode in the oven at 100 °C for 5 min to cure the epoxy (Figure 1).

Electrode Modification

1. Conduct the film deposition by cyclic voltammetry using a three-electrode arrangement (cell 1 in the main text) so that the polymer reduction current reaches 60–100 μA at 0.1 V/s (Figure 1b). Typically, the potential of a pencil-lead electrode is cycled 6 times between 0 V and the potential where the monomer oxidation current reaches 0.4 mA. The final potential is set to 0 V to obtain a neutral POT film. After POT deposition, wash the modified electrode with acetonitrile.

2. Prepare a 1 mL THF solution containing 8 mg of PVC, 31 μL of *o*NPOE, and 4.4 mg of TDDATFAB.

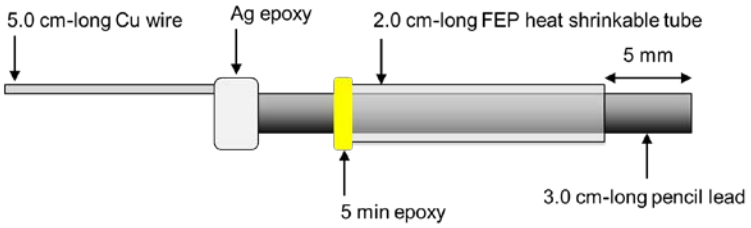

Figure 4-4. Design of an unmodified pencil lead electrode.

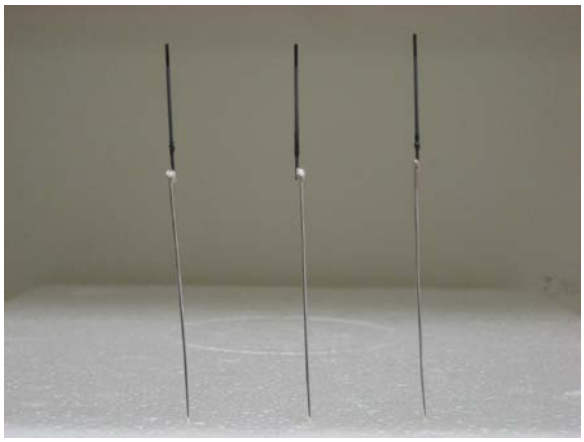

Figure 4-5. Drying PVC/POT-modified electrodes directed upward.

3. Immerse a POT-modified pencil lead (~1.5 cm in depth) into the THF solution for 10 s. Remove the electrode from the solution and direct the immersed end upward to drain the THF solution from the tip (Figure 5). THF will completely evaporate within 5 min to remain a PVC membrane (Figure 2a).

Preparation of Standard Solutions

1. Following aqueous solutions were prepared with tap water collected from the cold water tap of a laboratory sink after the water was allowed to run for 15 min.

2. Prepare 250 mL of 1 mM Li_2SO_4 by weighing out 27.49 mg of solid Li_2SO_4 and dissolving it in 250mL water using a volumetric flask.

3. Prepare 50 mL of 1 mM $LiClO_4$ by weighing out 5.32 mg of solid $LiClO_4$ and dissolving it in 50 mL of 1 mM Li_2SO_4 using a volumetric flask. Dilute 1.00 mL of the 1 mM $LiClO_4$ stock solution with 50 mL of 1 mM Li_2SO_4 to prepare 20 µM $LiClO_4$ in 1 mM Li_2SO_4.

4. Dilute 50, 150, 300, 400, and 500 µL of the 20 µM $LiClO_4$ solution with 10 mL of 1 mM Li_2SO_4 solution to prepare 5 other standard solutions containing approximately 100, 300, 600, 800, 1000 nM $LiClO_4$ (see Table 1 for accurate concentrations).

Stripping Voltammetry

1. The instrument is CHI 600A electrochemical workstation equipped with Faraday cage for stripping voltammetry measurements. Use a three-electrode arrangement with a double-junction Ag/AgCl reference electrode (BASi, West Lafayette, IN) and a Pt-wire counter electrode (cell 2 in the main text).

2. Measure a cyclic voltammogram with the 1 mM Li_2SO_4 background solution to find the anodic potential where the current reaches to –0.6 μA (Figure 6). The optimum preconcentration potential is 10–30 mV more positive in comparison to this potential.

3. Use 5 min preconcentration time and record a stripping voltammogram of 1 mM Li_2SO_4 until stable background voltammograms are obtained. With a typical electrode, the fist two background voltammograms overlap with each other very well.

4. Record the stripping voltammogram of each $LiClO_4$ solution with 5 min preconcentration (Figure 3a).

Data Analysis for Standard Solutions and Spiked "Unknown" Samples.

1. Carry out the least-square analysis of peak currents versus perchlorate concentrations in standard solutions (Table 2) to determine slope, *m*, intercept, *b*, and standard deviation about regression, s_r, as given by (*N* is the number of standard solutions)

$$m = \frac{\sum x_i y_i - \frac{\sum x_i \sum y_i}{N}}{\sum x_i^2 - \frac{\left(\sum x_i\right)^2}{N}} = 0.5358 \qquad \text{(S-1)}$$

$$b = \frac{\sum y_i - m\sum x_i}{N} = 0.1706 \qquad \text{(S-2)}$$

$$s_r = \sqrt{\frac{\sum y_i^2 - \frac{\left(\sum y_i\right)^2}{N} - m^2\left[\sum x_i^2 - \frac{\left(\sum x_i\right)^2}{N}\right]}{N-2}} = 0.0117 \qquad \text{(S-3)}$$

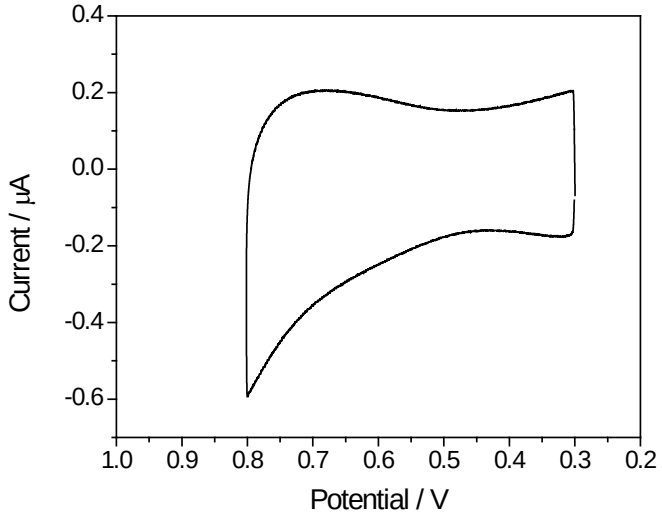

Figure 4-6. Background CV of a PVC/POT-modified pencil lead electrode in 1 mM Li_2SO_4. Scan rate, 0.1 V/s.

Table 4-2. Analytical Results of Standard Solutions

concentration, x_i, µM	peak current, y_i, µA	x_i^2	y_i^2	$x_i y_i$
0.100	0.236	0.0100	0.055696	0.0236
0.296	0.323	0.0874	0.104329	0.0955
0.488	0.420	0.2380	0.176400	0.2049
0.769	0.580	0.5917	0.336400	0.4462
0.952	0.690	0.9070	0.476100	0.6571
2.604	2.249	1.8341	1.148925	1.4272

2. Measure a peak current, y_u, of a spiked "unknown" sample and calculate the corresponding concentration, x_u, and its standard deviation, s_u, using the calibration curve (Table 3) and the following equations.

$$x_u = \frac{y_u - b}{m} \tag{S-4}$$

$$s_u = \frac{s_r}{m}\sqrt{1 + \frac{1}{N} + \frac{\left(\frac{\sum y_i}{N} - y_u\right)^2}{m^2\left[\sum x_i^2 - \frac{\left(\sum x_i\right)^2}{N}\right]}} \tag{S-5}$$

INSTRUCTOR NOTES

1. Information about hazards is given in the main text and student instructions.

2. Preparation of TDDATFAB is not included in the 3–4 hour laboratory session. This salt can be prepared in a large scale (5–10 g) and stored in a refrigerator.

Table 4-3. Analytical Results of Spiked Samples

	sample 1	sample 2	Sample 3
spiked concentration, µM	0.392	0.583	0.676
measured peak current, y_u, µA	0.383	0.484	0.543
calculated concentration, x_u, µM[a]	0.40	0.58	0.69
standard deviation, s_u, µM[a]	0.02	0.02	0.02

[a] Calculated using the results of the least-square analysis of the data in Table 2.

REFERENCES

(1) Sellers, K.; Weeks, K. R.; Alsop, W. R.; Clough, S. R.; Hoyt, M.; Pugh, B.; Robb, J., *Perchlorate: Environmental Problems and Solutions.* Taylor and Francis: Boca Raton, FL, **2007**.

(2) *Health Implications of Perchlorate Ingestion*; National Academies Press: Washington, DC, **2005**.

(3) Hecht, M. H.; Kounaves, S. P.; Quinn, R. C.; West, S. J.; Young, S. M. M.; Ming, D. W.; Catling, D. C.; Clark, B. C.; Boynton, W. V.; Hoffman, J.; DeFlores, L. P.; Gospodinova, K.; Kapit, J.; Smith, P. H. *Science* **2009**, *325*, 64−67.

(4) Kounaves, S. P.; Stroble, S. T.; Anderson, R. M.; Moore, Q.; Catling, D. C.; Douglas, S.; McKay, C. P.; Ming, D. W.; Smith, P. H.; Tamppari, L. K.; Zent, A. P. *Environ. Sci. Technol.* **2010**, *44*, 2360−2364.

(5) EPA Perchlorate. http://water.epa.gov/drink/contaminants/unregulated/perchlorate.cfm (accessed July 2012).

(6) Samec, Z.; Samcová, E.; Girault, H. H. *Talanta* **2004**, *63*, 21−32.

(7) Bendikov, T. A.; Harmon, T. C. J. *Chem. Educ.* **2005**, *82*, 439−441.

(8) Goldcamp, M. J.; Underwood, M. N.; Cloud, J. L.; Harshman, S.; Ashley, K. *J. Chem. Educ.* **2008**, *85*, 976−979.

5.0 IONOPHORE SYNTHESYS FOR ELECTROCHEMICAL RECOGNITION AT LIQUID/LIQUID MICROINTERFACES

This work has been published as P. J. Rodgers P. Jing, Y. Kim, and S. Amemiya. *J. Am. Chem. Soc.* **2008**, *130*, 7436–7442 and also as P. Jing, Y. Kim, and S. Amemiya, *Langmuir.*, **2009**, *25*, 13653-13660.

Ionophores were synthesized to investigate the interfacial recognition and extraction of heparin and low-molecular-weight heparin at nitrobenzene/water microinterfaces. A synthetic heparin mimetic, Arixtra is electrochemically extracted from the water phase into the bulk nitrobenzene phase containing highly lipophilic ionophores, methyltridodecylammonium **1** or dimethyldioctadecylammonium **2**.[1] Moreover, octadecylammonium **3**–**4** and octadecyl-guanidinium **5** are introduced as new, simple ionophores to model recognition sites of heparin-binding proteins at liquid/liquid interfaces. A new heparin ionophore **6**, 1-[4-(dioctadecylcarbamoyl)butyl]guanidinium, is the first to enable the voltammetric extraction of various polyanionic heparins with average molecular weights of up to ~20 kDa including those in commercial preparations (i.e., Arixtra (1.5 kDa), Lovenox (4.5 kDa), and unfractionated heparin (15 kDa), as well as chromatographically fractionated heparins (7, 9, 15, and 20 kDa)).[2]

TFAB salts of quaternary ammonium ionophores **1**–**3** and a supporting electrolyte TDDA were prepared as reported previously.[9] TFAB salts of octadecylammonium **4** or

octadecylguanidinium **5** were prepared by metathesis of KTFAB and octadecylguanidinium *p*-toluenensulfonate or octadecylamine hydrochloride in methanol. A dichloromethane solution of the mixture was washed several times with deionized water. The solvent was removed by rotary evaporator and the product was dried further under vacuum. Octadecylguanidinium *p*-toluenensulfonate was synthesized and characterized as described elsewhere.[21]

The TFAB salt of 1-[4-(dioctadecylcarbamoyl)butyl]guanidinium **6** or N,N-dioctadecyl-guanidinium **7** was prepared by metathesis of KTFAB in ethanol and the p-toluenesulfonate or lactate salt of the respective ionophores in dichloromethane as reported for preparation of TFAB salts of the other ionophores investigated in this work.[21] The p-toluenesulfonate salts of ionophore **6**[51] and octadecylguanidinium[52] and the lactate salt of ionophore **7**[53] were synthesized and characterized by ^{1}H NMR as described below.

Scheme 5-1. Structure of Ionophores **1**-**7**

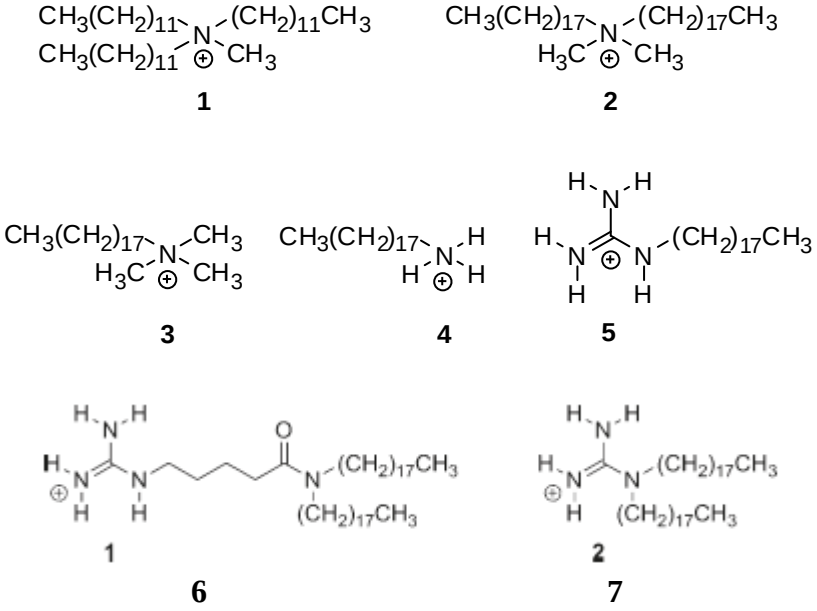

A 1,2-DCE solution of Arixtra-ionophore **6** complexes was obtained by anion exchange between *p*-toluenesulfonate of the ionophore **6** salt in a 1,2-DCE solution and Arixtra in a dialyzed solution. Specifically, a 200 μL 1,2-DCE solution of 3 mM p-toluenesulfonate salt of ionophore **6** and 0.1 M TDDATFAB was washed three times with an 800 μL aqueous solution of 0.4 mM Arixtra and 1 mM HEPES at pH 7.0. The resulting 1,2-DCE solutionwas directly used for cyclic voltammetric experiments.

1-[4-(Dioctadecylcarbamoyl)butyl]guanidinium ptoluenesulfonate. The p-toluenesulfonate salt of ionophore **6** was synthesized as reported by Kunitake and co-workers.[S1] ^{1}H NMR ($CDCl_3$, δ) 0.89 (t, J = 6.6 Hz, $–CH_2(CH_2)_{16}CH_3$, 6H), 1–1.9 (m, $–CH_2(CH_2)_{16}CH_3$ and $CH_2CH_2CH_2NH$, 68H), 2.3–2.5 (br, $CH_2C(O)$ and $ArCH_3$, 5H), 3.1–3.4 (m, $–CH_2(CH_2)_{16}CH_3$ and $CH_2CH_2CH_2NH$, 6H), 6.9–7.1 (br s, NH_2 and NH, 5H), 7.17 (d, J = 8.1 Hz, Ar H, 2H), and 7.73 (d, J = 8.1 Hz, Ar H, 2H).

N,N-dioctadecylguanidinium lactate. The lactate salt of ionophore **7** was synthesized as follows.[S2] 50 mg L(+)-lactic acid in 0.3 mL *n*-butanol was added to a solution of 500 mg *N,N*-dioctadecylamine in 1.5 mL *n*-butanol at 60 °C. The mixture was stirred at 120 °C for 3 hours. Then, 47.3 mg cyanide dissolved in 0.5 mL *n*-butanol was added to the mixture. After the mixture was stirred for 3 hours at 120 °C, the crude product was precipitated in acetone, filtered, and washed with diethyl ether several times. The final product (400 mg, 64 %) was dried further under vacuum. ^{1}H NMR ($CDCl_3$, δ) 0.89 (t, J = 6.4 Hz, $–CH_2(CH_2)_{16}CH_3$, 6H), 1.2–1.7 (m, $–CH_2(CH_2)_{16}CH_3$ and $–CH(OH)CH_3$, 67H), 2.5–3 (br s, NH_2 and NH, 5H), 3.1–3.4 (m, $–CH_2(CH_2)_{16}CH_3$ and $–CH(OH)CH_3$, 5H), and 4.2 (m, $–CH(OH)CH_3$, 1H).

1- Octadecylguanidinium p-toluenesulfonate. The *p*-toluenesulfonate salt of ionophore **7** was synthesized as reported by Kunitake and co-workers.[S3] ^{1}H NMR (DMSO-d_6, δ) 0.84 (t, J = 6.6 Hz, –$CH_2(CH_2)_{16}CH_3$, 3H), 1–1.5 (m, –$CH_2(CH_2)_{16}CH_3$, 32H), 2.28 (s, $ArCH_3$, 3H), 3.05 (q, J = 6.6 Hz, –$CH_2(CH_2)_{16}CH_3$, 2H), 6.6–7.4 (br s, NH_2 and NH, 5H), 7.1 (d, J = 8.1 Hz, Ar H, 2H), and 7.46 (d, J = 8.1 Hz, Ar H, 2H).

REFERENCES

(1) Rodgers, P. J., Jing, P., Kim, Y., Amemiya, S., *J. Am. Chem. Soc.* **2008**, *130*, 7436–7442.

(2) Jing, P., Kim, Y., Amemiya, S., *Langmuir.*, **2009**, *25*, 13653-13660.